**DRAFT**

# Analysis of Sensitivity of Plain Jointed Concrete Pavement in California to Early-age Cracking using HIPERPAV

Report Prepared for

**CALIFORNIA DEPARTMENT OF TRANSPORTATION**

By

**E. B. Lee, V. Lamour, J. H. Pae, and J. Harvey**

**August 2003**

**University of California**
**Pavement Research Center**

**TABLE OF CONTENTS**

**LIST OF FIGURES**

**LIST OF TABLES**

# 1.0 INTRODUCTION

Concrete is made from the mixing of hydraulic cement, water, and aggregate. The mixing of the cement and water initiates a reaction that results in the conversion of the cement powder and water into a solid crystalline paste, which gains strength as the reaction proceeds. The reaction is exothermic, meaning that it releases heat. The heat is transmitted to the atmosphere and the soil beneath the slab at a rate that is dependent on the properties of the mix, the thickness of the slab, the atmospheric conditions above the slab, and the condition and properties of the soil below the slab.

The reaction initially accelerates. The reaction begins to decelerate as the amount of unreacted cement in the mix decreases, and as the mix solidifies causing the rate of contact between free water and unreacted cement to decrease. As the reaction proceeds, the concrete continuously gains strength due to the conversion of cement and water into hardened crystals, assuming that cracks don't develop.

The concrete can be thought of as consisting of three phases. The cement paste bonds to the aggregate particles in the mix, cementing them together, with the cement paste and aggregate forming the first two phases in the concrete. The third phase is the transition zone between the aggregate particles and the cement paste. This transition zone typically has weaker strength than the paste itself.

## 1.1 Thermally Induced Tensile Stresses

Different types and grinds of cement have different strength gain and heat development rates. Types of cement include several types of portland cement, which primarily relies on various types of calcium silicate hydrate, calcium aluminates, and calcium hydroxide for its strength; calcium sulfoaluminates; and calcium aluminates. The various types of cement have

various strength gain rates depending on their chemical composition, the size of the cement particles, admixtures, and the proportions of cement, water, and aggregate in the mix. Aggregate type also plays a significant role in concrete strength and a lesser role in heat absorption and transmission. Aggregate type primarily controls the coefficient of thermal expansion and contraction of the concrete, which is a property that relates thermally induced strains to temperature changes in the concrete.

As the cement reacts and the temperature increases within a concrete slab, the slab expands. Then, as the generation of heat from the exothermic reaction reaches its maximum, the slab begins to cool and it contracts (this is sometimes referred to as *thermal shrinkage*). By the time the temperature of the slab reaches its maximum, the slab has also gained considerable stiffness and strength. As the slab cools, the slab contraction is restricted by friction at the slab/base interface, with higher friction causing greater resistance to the contraction and greater stresses in the slab. Assuming the concrete has no creep to relieve the stresses, the tensile stress midway along the longest dimension of the slab can be calculated using the equation:

$$\sigma_t = E_c \cdot \alpha \cdot \Delta T \cdot f \cdot L/2 \qquad \textbf{(1)}$$

where $\sigma_t$ is the tensile stress in the concrete
$E_c$ is the elastic stiffness of the concrete
$\alpha$ is the coefficient of thermal expansion (strain/temperature change)
$\Delta T$ is the change in temperature (cooling from peak temperature)
$f$ is the friction between the slab and the base
$L$ is the length of the longest dimension of the slab.

If the tensile stress exceeds the tensile strength during the simultaneous processes of strength gain, stiffness gain, and expansion followed by contraction, the slab is likely to crack.

It can be seen from Equation 1 that low stiffness, low coefficient of thermal expansion (primarily controlled by the coefficient of thermal expansion of the aggregate), small

temperature changes, low friction between the base and slab, and short slab lengths all contribute to reduce tensile stresses. Because the stiffness and strength of the cement paste are both gained through the same chemical process, decreasing the stiffness of the mix may not achieve the desired result of reducing the risk of cracking. The stiffness and strength of the mix are also controlled in large part by properties of the aggregate, including its stiffness, strength, shape, and texture.

The tensile stresses estimated by Equation 1 caused by uniform contraction of the slab are generally assumed to be uniform between the top and bottom of the slab. Stresses within the slab are also caused by differences in expansion and contraction between the top and bottom of the slab. These differences result in slab curling, which changes the relative support conditions at the edges and the center of the slab. The surface of the slab is exposed to climatic effects (air, wind, and solar radiation) and typically undergoes greater temperature changes than the bottom. The bottom of the slab is insulated from these climatic effects by the relatively constant temperature of the material beneath the slab and by the slab itself.

These differences between the top and bottom of the slab result in vertical temperature gradients within the slab, typically causing it to be hotter at the surface than at the bottom during the day, and cooler at the surface than at the bottom during the night. The difference in support due to the slab curling, which can sometimes result in the edges of the slab lifting off of the base, causes stresses in the slab due to gravity acting on the mass of the slab and pushing the lifted region of the slab back towards the base. As shown in Figure 1, if the top of the slab is cooler, the edges of the slab lift up and the mass of the slab is primarily supported by the center of the slab. Gravity pushing the edges down results in tensile stresses at the top of the slab. As shown in Figure 2, if the top of the slab is hotter, the center of the slab lifts up and the mass of the slab

is carried to a greater degree by the corners. Gravity pushing down on the slab causes tensile stresses at the bottom of the slab. These tensile stresses are to some degree additive with the uniform expansion tensile stresses described previously.

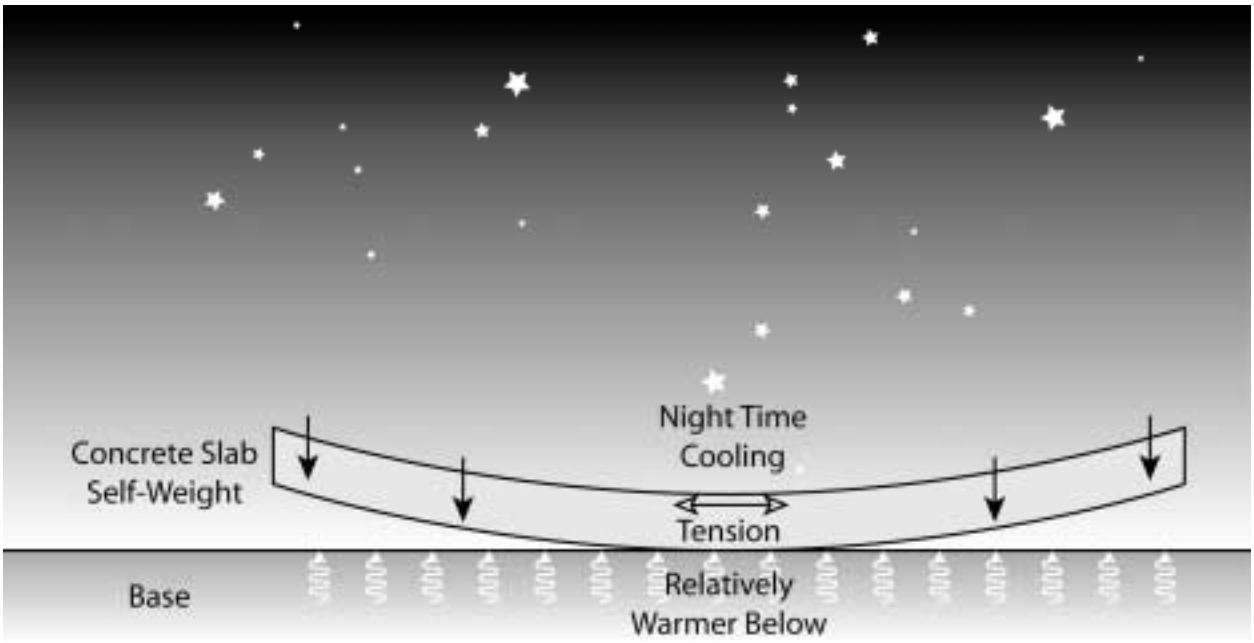


**Figure 1. Stresses caused by temperature gradient with slab top cooler than bottom.**

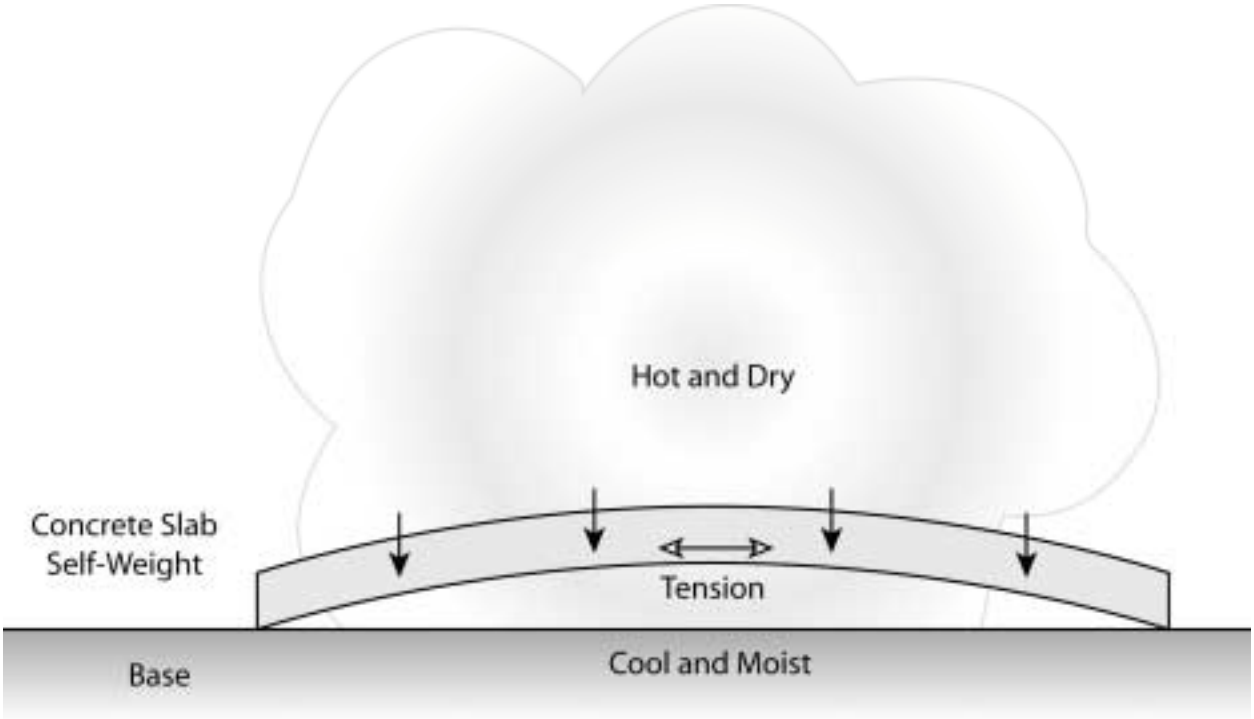


**Figure 2. Stresses caused by temperature gradient with slab top hotter than bottom.**

An early, simplified equation for estimating curling stresses at the mid-slab edge is (*1*):

$$\frac{\sigma_t = C \cdot E_c \cdot \alpha \cdot \Delta T}{(1-\nu^2)} \quad \textbf{(2)}$$

where

$\sigma_t$ is the tensile stress in the concrete
$C$ is a factor that accounts for slab length and thickness, and subgrade stiffness
$E_c$ is the elastic stiffness of the concrete
$\alpha$ is the coefficient of thermal expansion (strain/temperature change)
$\Delta T$ is difference in temperature between the top and bottom of the slab
$\nu$ is the Poisson's ratio

The factor for slab dimensions and length is a function of $L/l$, where $L$ is the slab length and $l$ is the radius of relative stiffness of the slab/subgrade system. The radius of relative stiffness is defined as:

$$l = \left[Eh^3/\left(12\left(1-\nu^2\right)k\right)\right]^{0.25}$$

where:

$E$ is the elastic stiffness of the concrete
$h$ is the thickness of the concrete
$\nu$ is the Poisson's ratio of the concrete
$k$ is the modulus of subgrade reaction (a measure of base/subgrade stiffness)

$C$ goes to zero as $L/l$ goes to zero, and $C$ goes to 1.1 as $L/l$ goes to 8. Therefore, the curling stress equation indicates that tensile stresses are reduced by less stiff concrete ($E_c$), smaller temperature gradients ($\Delta T$), smaller slab lengths ($L$), smaller coefficients of thermal expansion ($\alpha$), and less stiff support to the slab ($k$). A less stiff base allows the base to deform more with the deformations of the slab, maintaining more uniform support between slab and base and reducing stresses. Curling due to temperature gradients can be tracked by temperature measurements and follow a typical day-to-night cycle.

## 1.2 Shrinkage Induced Tensile Stresses

In addition to temperature changes, the hydrating cement and the mix undergo two types of shrinkage:

- drying shrinkage caused by the loss of water, primarily from the surface of the wet mix and later the surface of the slab as it solidifies, and
- autogenous shrinkage, which is a decrease in volume that occurs when water and dry cement react to become crystalline cement paste.

Uniform shrinkage throughout the slab results in a contraction, which is resisted by friction with the base, as with temperature related contraction.

Drying shrinkage is typically not uniformly distributed within the slab. The surface of the slab typically dries faster and more than the bottom of the slab because of interaction with wind, lower humidity, and higher temperatures at the slab surface. The typical drying shrinkage gradient from top to bottom in a slab results in a shape change to the slab similar to that caused by nighttime temperature gradients, that is, lifting of corners and an overall convex shape when viewed from above (Figure 1). Gravity pushing down on the uplifted parts of the slab, in this case the edges, causes tensile stresses, just as occurs for temperature induced slab shape changes.

In this report, shape changes induced by vertical moisture gradients in the slab are referred to as *warping*. These changes typically do not vary much day to night, as do temperature gradients, but typically increase from construction. The size of the moisture gradient typically varies somewhat from wet season to dry season. Shrinkage and shrinkage gradients follow a seasonal pattern with an underlying monotonic increase as hydration continues.

Tensile stresses caused by uniform shrinkage, and shrinkage-gradient induced warping are additive with tensile stresses caused by uniform changes and temperature gradient induced curling. Less stiff bases offer similar benefits in reducing tensile stresses from shrinkage and temperature changes. Higher strength concrete reduces the risk of cracking, as does shorter slab length. Construction practices that reduce differences in moisture, and therefore shrinkage between the surface and the bottom of the slab are extremely important as well. These practices include sealing the surface of the concrete and protecting it from heat and wind. Saw cutting of transverse and longitudinal joints as soon as the concrete is strong enough to support the equipment and provide clean cuts also reduces the risk of temperature- and shrinkage-induced cracking by relieving tensile stresses caused by contraction.

## 1.3 Tradeoffs between Strength, Stiffness, and Stresses

Tradeoffs exist between strength, stiffness, and tensile stresses. Early-age cracking occurs when tensile stresses exceed tensile strength in the concrete. However, the "easy" solution of increasing the strength of the concrete, or reducing the stiffness of the concrete, does not solve the problem. The task of optimizing a pavement for early-age cracking resistance is more complex and requires a more careful and complete analysis, which is the objective of the HIPERPAV software. The factors involved include:

- concrete stiffness, which results in greater tensile stresses, increases with concrete strength,
- temperature increases from the reaction of cement and water are usually greater for concrete mixes that gain strength rapidly, which increases the amount of eventual thermal contraction and temperature gradients and therefore increases tensile stresses,

- drying shrinkage and drying shrinkage gradients that cause warping, which result in greater tensile stresses, usually increase with concrete strength.

The first key to reducing the risk of early-age cracking is to balance increased concrete strength, which reduces the risk, with increased temperature gain and drying shrinkage, which both increase the risk. This balance is achieved in the concrete mix design through materials selection, proportioning, and admixtures.

The second key to reducing the risk of early-age cracking is to understand and take advantage of construction practices that reduce the risk, for example, timely saw cutting of joints, curing practices, and timing of construction for different climates.

## 1.4 Importance of Predicting and Mitigating Early-age Cracking

Cracking is one of the primary design and construction concerns for concrete pavement. Cracks shorten the effective life of the pavement. Cracks lead to increased maintenance and rehabilitation costs for the agency because they increase the roughness of the pavement, and because they are expensive and difficult to maintain.

Concrete pavements are expected to provide many years of service with very low maintenance costs, so it is particularly important to prevent early-age cracks. If early-age cracks occur, increased maintenance and eventually rehabilitation may be necessary from the beginning of the life cycle of the pavement.

## 1.5 HIPERPAV Software

A computer program (HIPERPAV) has been developed under a Federal Highway Administration (FHWA) research contract to predict early-age behavior of jointed concrete

pavements.(*2*) HIPERPAV is a design and construction analysis tool for engineers to predict and prevent cracking in the first 72 hours following the placement of new concrete. HIPERPAV contains algorithms to model the parameters that influence the behavior of the concrete pavement. These are grouped into the following four categories (*1, 3, 4*):

- Mix Design Parameters:
  - cement type
  - lab maturity data
  - coarse aggregate type
  - cement content
  - silica fume / fly ash content
  - water content
  - coarse / fine aggregate content
  - use of water reducer
  - use of retarder
  - use of accelerator
- Pavement Design:
  - subbase type
  - subbase friction
  - transverse joint spacing
  - PCC flexural strength
  - PCC modulus of elasticity
  - slab thickness

- Construction Parameters:
  - curing method
  - time of day of construction
  - initial PCC mix temperature
  - age of concrete at time of opening to traffic
  - age of concrete at time of saw cutting
  - initial subbase temperature
- Environmental Parameters:
  - air temperature
  - temperature distribution
  - relative humidity distribution
  - solar radiation
  - average wind speed

The program prompts the user to provide data for a series of four input screens (design inputs, mix design inputs, environmental inputs, and construction inputs), as shown in Figure 3. The program provides default values for many variables if the user does not have input data. Data may be entered in inch-pound or metric units, and the user can switch to English or Metric units for each input screen or for individual values as desired. Once all the input parameters have been defined, HIPERPAV analyzes the input values using a series of prediction equations and presents a graph comparing the tensile stresses caused by temperature and drying shrinkage changes with strength development over the initial 72-hour period after placement, as shown in Figure 4.


**Figure 3. HIPERPAV main input screen.**

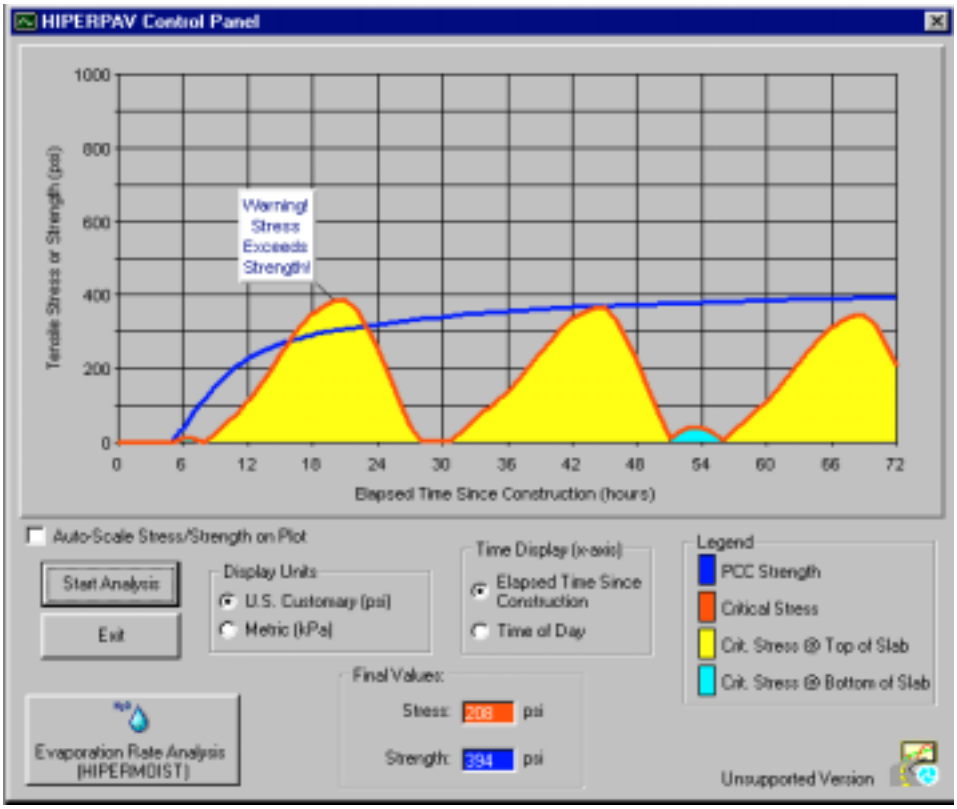


**Figure 4. HIPERPAV output screen.**

The output is intended to provide the engineer with information necessary to determine whether there is potential problem with early-age cracking (*4*).

## 1.6 FHWA Validation of HIPERPAV

The FHWA has reported extensive validation of HIPERPAV for a range of design, materials, and climatic conditions for several sites in the United States.(*4*) The validation process included the instrumentation of pavements under construction with the objective of studying how those pavements would behave at early ages. The FHWA reports that the validation results demonstrated an excellent predictive capability for HIPEPRAV for the overall early-age behavior. The FHWA reported that the overall system was found to predict crack formation with an average error of 5.4 hours, meaning that cracks appeared within 5.4 hours of the prediction of cracking by HIPERPAV using the 50 percent reliability feature of the software.

This validation was for cracks at sawed joints, while HIPERPAV predicts cracking in the middle of an uncut slab. The FHWA researchers used "stress magnification factors" to account for the difference between observed cracking at the sawed joints and cracking predicted by HIPERPAV at the middle of an uncut slab. The states in which full-scale validation was performed include Minnesota, Nebraska, Arizona, Texas, and North Carolina.(*4*)

On some of the projects included in the validation study, HIPERPAV did not predict cracking because the predicted tensile stress was not greater than the predicted tensile strength. On those projects, the researchers assumed that cracking was predicted by HIPERPAV at the time when the ratio of stress over strength was maximum in the 72-hour prediction period.(*4*) The use of the ratio of stress over strength from HIPERPAV predictions is discussed in greater detail in Chapter 3 of this report.

## 1.7 Research Objectives

The California Department of Transportation (Caltrans) is interested in the prediction of early-age cracking and the development of effective mitigation measures for early-age cracking. Caltrans is currently using new concrete pavement to reconstruct many portland cement concrete (PCC) and asphalt concrete freeway pavements originally built in the 1950s and 1960s. More work of this type is expected over the next decade. Early-age cracking has developed on some recent Caltrans projects.

A plan for a multi-stage research program has been developed by the University of California Pavement Research Center (UCPRC) for the investigation of early-age cracking.(*5*) The plan includes the following objectives:

1. Evaluation of HIPERPAV software, including a critical review of the models in the software, and a sensitivity study of the relative effects of variables included in HIPERPAV on early-age cracking for California conditions,
2. Field Validation of HIPERPAV in California, including instrumentation and monitoring of slabs on four sites in the California desert, and
3. Development of recommendations for the mitigation of early-age cracking and the use of HIPERPAV in California.

## 1.8 Scope of this Report

The work included in this report completes the first of the three objectives of the early-age cracking investigation plan. This report also presents preliminary recommendations for the use of HIPERPAV and for the mitigation of early-age cracking based on the HIPERPAV sensitivity analysis.

The results of the field validation from the four field sites (second objective) will be included in a report to be written after the construction of the four projects. This report is expected to be completed by early 2004.

Chapter 2 presents a critical review of the models included in the HIPERPAV software. Chapter 3 describes the experiment factorial design for the sensitivity study and the development of the input data. Chapter 4 presents an analysis of the sensitivity study results, and Chapter 5 presents conclusions and preliminary recommendations.

## 2.0 REVIEW AND CRITIQUE OF HIPERPAV MODELS

HIPERPAV software models early-age behavior of JPC subjected to stresses from moisture and thermal changes. In short, it includes a finite element based PCC temperature development model, which accounts for heat generation from the hydrating paste, solar radiation, insulation, surface convection, dynamic specific heat, and thermal conductivity values. Several mechanical properties are also modeled including thermal coefficient of expansion, drying shrinkage, and creep relaxation. The PCC strength and modulus of elasticity are predicted using Arrhenius-based maturity methods. Finally, the critical pavement stresses are predicted using a complex closed-form solution based on engineering mechanics. Additional restraint to free movement due to slab-base friction and curling are also modeled directly.

The basic algorithm for the early crack prediction is shown in Figure 5. The temperature profile in the JPC is obtained from the resolution of a two-dimensional transient heat transfer problem by a finite element model. The drying shrinkage profile is assumed to be linear between the mid-depth of the JPC, below which there is assumed to be no drying effect, and the surface of the JPC, where the maximum drying shrinkage is calculated from the maturity of the concrete using the RILEM model.(*4*)

The concept used for the maturity calculation is that of equivalent age, that is, the age at the reference temperature (20°C) at which the same proportion of the ultimate strength is reached as would occur at other temperatures. Using this method, HIPERPAV defines the initial time for the mechanistic problem, meaning the time when stress begins to develop, as the time when concrete is set with a degree of hydration of 0.43 times the water-cement ratio. The creep relaxation is then modeled through a reduced elastic modulus that allows the calculation of the stresses with an explicit equation relating strains (thermal and drying strains) to stresses

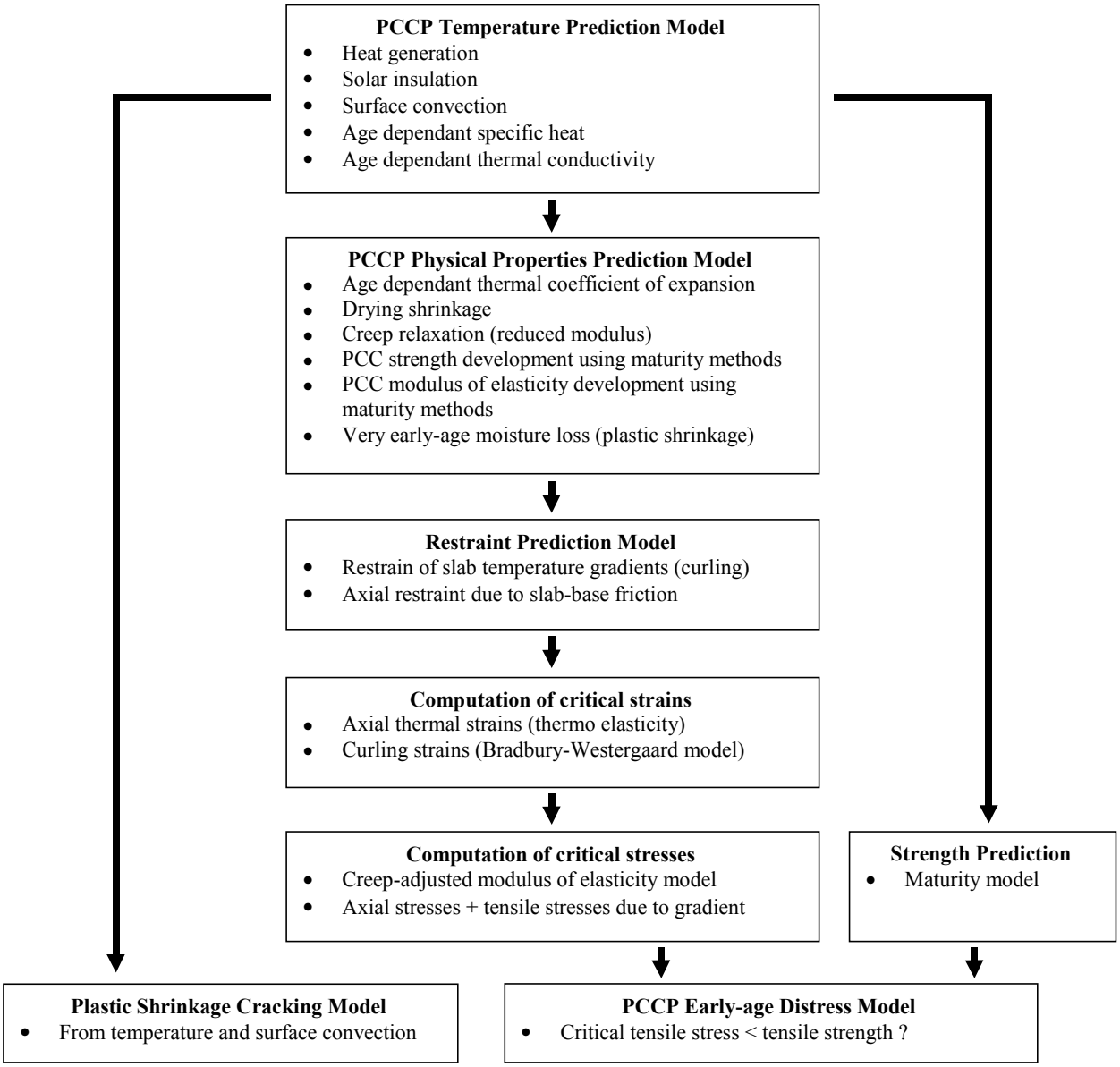


**Figure 5. Algorithm for HIPERPAV prediction of early-age cracking.(*3*)**

elastically. This is primarily done by adding elastic curling stresses (Bradbury-Westergaard model (*1*) to axial stresses caused by thermal and drying strains.

Finally, the graph of the maximum tensile stress over time, occurring at either the bottom or top of the JPC, is compared to the graph of the tensile strength of the concrete. When the critical stress reaches the strength of the concrete, HIPERPAV predicts the occurrence of cracking.

## 2.1 Modeling Issues for Early-age Cracking Prediction in Jointed Plain Concrete Pavement (JPCP)

Early-age cracking in unloaded pavement or slabs is caused by the following successive phenomena:

a. **Volumetric Change:** shrinkage and temperature change in the concrete (Figure 6a).

b. **Creation of stresses due to a restraining support and/or gradients of deformation:** referred to in this report as *curling* when it is caused by temperature gradients and *warping* when it is caused by shrinkage gradients (Figure 6b).

c. **Fracture:** crack opening and propagation and partial release of the stresses (Figure 6c).

For each of these phenomena, the HIPERPAV model should take into account the major controlling factors. These phenomena are very complex. However, coupled with one another other due to hydration, drying shrinkage, fracture, and chemo-thermo-mechanical effects, a simplified approach based on experimental data can give a good prediction of the global phenomenon. Modeling of the key mechanisms of each of the phenomena is discussed in the following sections.

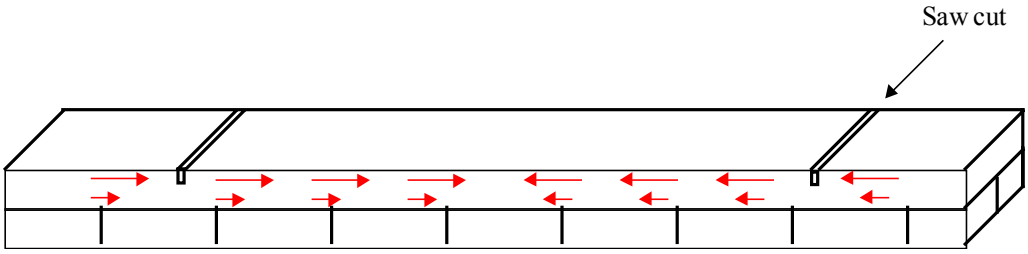


**Figure 6a. Volume change in the concrete.**

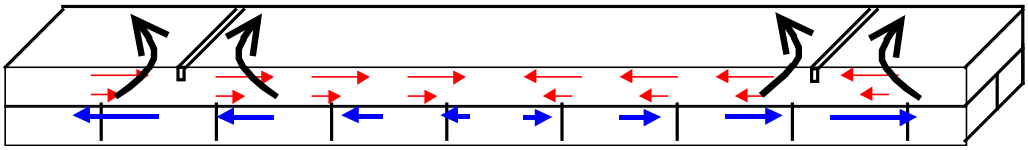

**Figure 6b. Tensile stress development due to restrain and deformation gradients.**

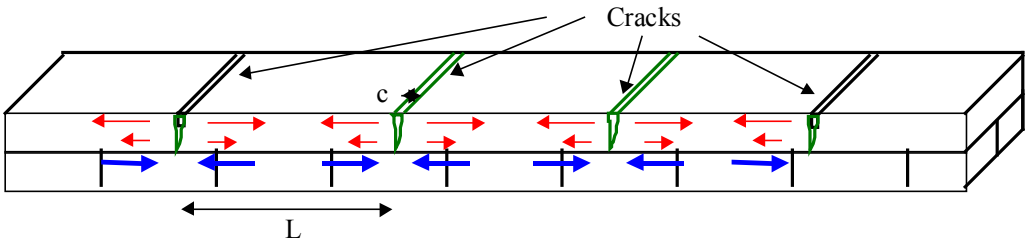


**Figure 6c. Fracture and partial stress release.**

**Figure 6. Early-age cracking in unloaded concrete pavement.**

2.1.1 Modeling Free Strain in the Concrete Pavement at Early Ages

Volume changes in concrete are caused by the following mechanisms:

- **Autogenous shrinkage over time and temperature.** Autogenous shrinkage is caused by the hydration of concrete. Autogenous shrinkage can be predicted from the mix design and typically ranges between 100 microstrain for normal strength concrete to 300 microstrain for high strength concrete.
- **Drying shrinkage over time (before and after setting).** Drying shrinkage is caused by the drying process, which is significantly controlled by the curing compound

applied to the surface of the slab and the timing of its application. Drying shrinkage is difficult to implement in a model because it is a three-dimensional transport phenomenon.

- **Thermal shrinkage over time.** Thermal shrinkage is caused by the temperature rise due to exothermic hydration from the reaction of the cement and water. As was discussed in Chapter 1, the concrete is less stiff when the temperature is rising, and has gained stiffness by the time the temperature has peaked and the concrete begins to cool. Thermal shrinkage can be predicted through a maturity approach that describes the kinetics of hydration.

It is clear that none of the models available in academic and industrial fields is able to quantitatively predict these three mechanisms of volume change without a prior calibration to empirical databases.

### 2.1.2 Modeling the Stresses due to Strains and Constraints

Constraints are generated by the friction between the concrete slabs and the supporting layer (rigid, soft, or multi-layered). The geometry of the pavement itself is also a constraint that particularly influences the curling and warping caused by temperature and shrinkage gradients. To calculate stresses from the free strains and constraints, it may be assumed that cracking has not yet occurred, meaning that stresses are released only by the effect of creep. A non-linear constitutive law based on viscoplasticity is necessary to account for creep for the most accurate prediction of the stress profile within the concrete pavement.

### 2.1.3 Modeling the Occurrence of Cracking and Damage

Instantaneous fracture can be predicted simplistically by comparing maximum tensile stress and tensile strength. However, this simplified model based on the tensile strength criterion works only if there are pure tensile stresses in the concrete. Further, the model only represents pre-failure. An incremental constitutive model with more complete yield functions and internal history variables is recommended when multiple stresses and cumulative damage occur in the material. Regarding early cracking in jointed plain concrete pavement (JPC), it is essential to predict cumulative damage over time in the first week to assess durability.

## 2.2 Strengths of HIPERPAV

HIPERPAV uses mechanistic-empirical procedures that combine pavement responses from analytical methods and performance data from pavement research and field observations. Though the model is simplified in order to provide a quick and comprehensible tool to the user, some phenomena are accurately predicted through complete model formulations. This is the case for temperature prediction in the JPC using a non-linear finite element procedure and prediction of the mechanical properties of concrete using a maturity approach.

Although the early-age cracking problem is extremely complex to model, HIPERPAV provides a tool for benchmarking different JPC variables. For example, the effects of time of sawing, curing, and time of day of construction can all be modeled. From this viewpoint, HIPERPAV may help the designer to recommend solutions that minimize the risk of early cracking problems.

## 2.3 Weaknesses/Limitations of HIPERPAV

Many assumptions used in HIPERPAV limit the ability of the model to predict cracking phenomena. Some of them could be improved without changing the time required for calculation; others would require sophisticated calculations that would not be possible on a desktop computer. Remembering the progress made by HIPERPAV in providing engineers with a desktop tool to evaluate various factors controlling the risk of early-age cracking, the following recommendations should be thought of as a suggestion list for further improvement of early-age cracking models for pavements.

#### *2.3.1.1 Prediction of volumetric change*

The Laboratoire Central des Ponts et Chausses (LCPC) in France has shown that by restraining a concrete slab over one meter with controls preventing drying and temperature increases, cracks always occur due to autogenous shrinkage even in early-age concrete in which high creep relaxes stresses.(*6*) This result strongly suggests that HIPERPAV should take the ultimate autogenous shrinkage in the concrete into account. This phenomenon is especially important for high performance concrete with low permeability properties for which autogenous shrinkage can be as high as 300 microstrain.

Drying shrinkage prediction should take into account the diffusion process of water through the concrete. HIPERPAV does not directly take into account the permeability of concrete and its bleeding rate, which limits its accuracy in modeling the drying behavior of concrete with fine mineral admixtures such as fly ash or silica fume.

Another volumetric change mechanism that could be implemented is the volumetric expansion caused by ettringite formation occurring in calcium sulfoaluminate cements meeting Caltrans specifications for Fast-Setting Hydraulic Cement Concrete (FSHCC).

#### *2.3.1.2 Constitutive law and damage prediction*

The simple explicit calculation of elastic stresses from free strains used by the HIPERPAV software cannot provide precise stress distributions for JPC. An implicit incremental stress-strain behavior model would better predict the stresses in the concrete, especially the softening behavior due to creep. The irreversible plastic strains due to creep or cracks should be integrated into the model to take the redistribution of stresses into account. At the micro-scale level, crack opening and propagation properties are currently not taken into account. These properties can be very different for different types of aggregates and mineral admixtures. Inclusion of these properties in the modeling would result in better predictions of early-age cracking.

Finally, the maturity concept is generally applicable to wet-cured concrete. However, the maturity concept does not incorporate the effect of relative humidity, which may limit the accurate prediction of the mechanical properties of the concrete. The assumption that maturity is uniform throughout the slab (used in HIPERPAV) may limit the scope of the analysis to slabs in which the hydration of the concrete is fairly uniform over the slab thickness. This assumption may not cause major problems, but should be evaluated in the field.

#### *2.3.1.3 Effect of traffic loading*

The calculation of stresses in HIPERPAV is based on an idealized analytical Bradbury-Westergaard model that does not take traffic loading into account. In the case of concrete mixes used for rapid repairs, such as those used for nighttime closures and 55- and 72-hour closures, external loads will certainly influence the early-age cracking pattern of the concrete. The use of a finite element method to compute stresses could allow the software to solve this problem as

well as to consider other types of pavement such as jointed plain concrete with dowels, JPC with tied shoulders, and continuously reinforced concrete pavement.

#### *2.3.1.4 Probabilistic approach*

Material properties, environmental conditions, and construction practices are stochastic processes. To assess the risk of early-age cracking, it is therefore critical to implement a more complete probabilistic approach in which input data are entered in terms of their expected probabilistic distributions and the output is returned in terms of a probability of early-age cracking. HIPERPAV currently does not take the variation of each input parameter into account. Such an approach would require a large number of calculations. However, the current computational speed of desktop computers makes the use of Monte Carlo simulation feasible, as an example of a method to account for variability. This approach would also make the calibration of HIPERPAV much more straightforward, because field performance data for early-age cracking is probabilistic by its nature, as are the input data for HIPERPAV collected from the field.

The stress and strength computed by HIPERAV are mean values. Based on these mean values, HIPERPAV uses a probabilistic approach to calculate a critical stress and critical strength as a function of the reliability as a user input.[1]

[1] The research team is not able to find any written statement except a couple of presentation slides from the software developer explaining the background or logic of the probabilistic approach, which seems to be hidden in the software.

#### *2.3.1.5 Limited to certain materials*

HIPERPAV cannot be used to evaluate mixes with very fast strength gain, such as Fast Setting Hydraulic Cement Concrete (FSHCC) and Type III mixes that reach 2.8 MPa (400 psi) flexural strength in four hours because it cannot accommodate the curing characteristics of such mixes.

# 3.0 SENSITIVITY STUDY OF HIPERPAV FOR CALIFORNIA CONDITIONS—EXPERIMENT FACTORIAL

## 3.1 Summary of Input Parameters

Variables for the HIPERPAV sensitivity analysis were selected for typical California concrete pavement scenarios. The variables fall into four categories:

- Pavement design variables,
- Mix design variables,
- Environmental (climate region) variables, and
- Construction variables.

Table 1 summarizes all of the variables included in this study. HIPERPAV permits the use of two design reliabilities: 50 and 84 percent. For this study, the HIPERPAV option of a design reliability of 50 percent was used, which means that the mean value of both the stress and strength curves was used by HIPERPAV to determine whether or not early-age cracking will occur.

## 3.2 Design Variables

The three design variables were: subbase type, joint spacing, and PCC slab thickness. The HIPERPAV software uses the relation for friction (restraint stress versus horizontal displacement) shown in Figure 7 for each of the three subbase types used in this study. As can be seen from the figure, a much greater friction is assumed for cement stabilized bases (CSB) than for asphalt concrete subbases. For this study, it was assumed that CSB, as defined in HIPERPAV, includes the Lean Concrete Base used by the California Department of Transportation.

**Table1 Summary of Variables and Factor Levels Included in Sensitivity Study**

| Category | Variable | Factor Levels | Total Cells |
|---|---|---|---|
| Design | Subbase Type (3) | HMAC-smooth; HMAC-rough; CSB | 18 |
| | Joint Spacing (3) | 2.7 m (9 ft.)<br>4.2 m (14 ft.)<br>5.7 m (19 ft.) | |
| | PCC Slab Thickness (2) | 229 mm (9 in.)<br>305 mm (12 in.) | |
| Mix Design | Cement Type (2) | Portland cement Type II<br>Portland cement Type III | 16 |
| | Aggregate Type (2) | Gravel<br>Granite | |
| | Target Flexural Strength for Mix Design (2 for each cement type) | For Type II mixes, at 10 days:<br>3.8 MPa (550 psi); 4.5 MPa (650 psi)<br>For Type III mixes, at 12 hours:<br>2.8 MPa (400 psi); 3.1 MPa (450 psi) | |
| | Fly Ash Content (2 for each cement type) | For Type II mixes: 15 %; 25 %<br>For Type III mixes: 0 %; 25 % | |
| Environmental Conditions | Climate Region (3, one representative weather station for each region) | South Coast (Los Angeles);<br>Desert (Daggett);<br>Bay Area (San Francisco) | 9 |
| | Construction Month (3) | February; May; September | |
| Construction | Curing Method (3) | None;<br>Double Coat of Curing Compound Liquid;<br>Burlap | 36 |
| | Starting Time (3) | 6 A.M.;<br>2 P.M.;<br>10 P.M. | |
| | Cure/Saw Cut Start Time (4 combinations of time to curing seal application, delay in saw cut time) | (0 hours, 0 hours);<br>(0 hours,24 hours);<br>(6 hours, 0 hours);<br>(6 hours, 24 hours) | |
| Total number of tests (1 Reliability case: 50 percent) | | | 93,312 |

Notes on HIPERPAV acronyms: HMAC = Hot Mix Asphalt Concrete; CSB = cement stabilized base

Four PCC slab thicknesses were included in the original plan for the sensitivity analysis. Preliminary analyses indicated that the two PCC slab thicknesses included in the experiment design, 229 mm (9 in.) and 305 mm (12 in.), had little effect on the results compared with other factors. As a result, the number of factor levels for PCC slab thickness was kept at two.

The 18 combinations of design variables were identified with codes as shown in Table 2.

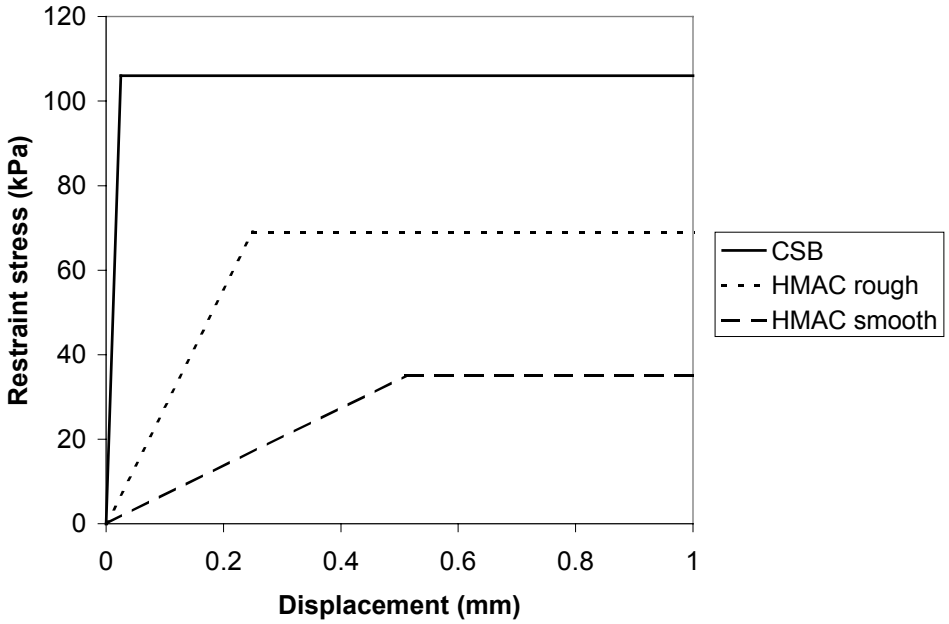


**Figure 7. Slab support-restraint model (after *3*).**

**Table 2 Summary of Design Variable Combinations**

| Code | Subbase* | Joint Spacing (m) | Thickness (mm) | Subbase Friction Force (kPa) | Subbase Movement at Sliding (mm) |
|---|---|---|---|---|---|
| D1 | HMAC-Smooth | 2.7 (9 ft.) | 229 (9 in.) | 34.5 (5 psi) | 0.51 (0.02 in.) |
| D2 | HMAC-Smooth | 2.7 (9 ft.) | 305 (12 in.) | 34.5 (5 psi) | 0.51 (0.02 in.) |
| D3 | HMAC-Smooth | 4.2 (14 ft.) | 229 (9 in.) | 34.5 (5 psi) | 0.51 (0.02 in.) |
| D4 | HMAC-Smooth | 4.2 (14 ft.) | 305 (12 in.) | 34.5 (5 psi) | 0.51 (0.02 in.) |
| D5 | HMAC-Smooth | 5.7 (19 ft.) | 229 (9 in.) | 34.5 (5 psi) | 0.51 (0.02 in.) |
| D6 | HMAC-Smooth | 5.7 (19 ft.) | 305 (12 in.) | 34.5 (5 psi) | 0.51 (0.02 in.) |
| D7 | HMAC-Rough | 2.7 (9 ft.) | 229 (9 in.) | 68.9 (10 psi) | 0.25 (0.01 in.) |
| D8 | HMAC-Rough | 2.7 (9 ft.) | 305 (12 in.) | 68.9 (10 psi) | 0.25 (0.01 in.) |
| D9 | HMAC-Rough | 4.2 (14 ft.) | 229 (9 in.) | 68.9 (10 psi) | 0.25 (0.01 in.) |
| D10 | HMAC-Rough | 4.2 (14 ft.) | 305 (12 in.) | 68.9 (10 psi) | 0.25 (0.01 in.) |
| D11 | HMAC-Rough | 5.7 (19 ft.) | 229 (9 in.) | 68.9 (10 psi) | 0.25 (0.01 in.) |
| D12 | HMAC-Rough | 5.7 (19 ft.) | 305 (12 in.) | 68.9 (10 psi) | 0.25 (0.01 in.) |
| D13 | CSB | 2.7 (9 ft.) | 229 (9 in.) | 103.4 (15 psi) | 0.025 (0.001 in.) |
| D14 | CSB | 2.7 (9 ft.) | 305 (12 in.) | 103.4 (15 psi) | 0.025 (0.001 in.) |
| D15 | CSB | 4.2 (14 ft.) | 229 (9 in.) | 103.4 (15 psi) | 0.025 (0.001 in.) |
| D16 | CSB | 4.2 (14 ft.) | 305 (12 in.) | 103.4 (15 psi) | 0.025 (0.001 in.) |
| D17 | CSB | 5.7 (19 ft.) | 229 (9 in.) | 103.4 (15 psi) | 0.025 (0.001 in.) |
| D18 | CSB | 5.7 (19 ft.) | 305 (12 in.) | 103.4 (15 psi) | 0.025 (0.001 in.) |

* CSB: Concrete Stabilized Base
HMAC-Rough: Hot Mix Asphalt Concrete, rough surface.

## 3.3 Mix Design Variables

Most of the properties of concrete depend on the interaction of many parameters, including water/cement ratio, cement content, admixtures, etc., that are usually correlated to each other and other properties. Rather than design a factorial for mix design variables that would result in many mixes that could never be produced in the field, it was decided to perform calculations to design two mixes for each cement type to meet typical project specifications. The four variables included in the mix design calculations were: cement type, aggregate type, target strength, and Type F fly ash content. There are four basic properties influenced by these variables that will be critical in the jointed plain concrete pavement cracking phenomenon:

- the kinetics of hydration of the cement,
- the total heat of hydration of the concrete,
- the ultimate strength of the concrete, and
- the ultimate thermo-elastic properties of the concrete.

These properties are discussed in the following sections.

### 3.3.1 Kinetics of Hydration of the Cement

The faster the cement hydrates, the greater the temperature of the concrete in the pavement due to the heat of hydration. Kinetics are of further importance when environmental conditions are considered, as shown in Figure 8.

Principally, the type of cement and the addition of mineral admixtures control the kinetics of hydration. Type II Portland cements are slow while Type III Portland cements are fast. The addition of a fly ash admixture slows the hydration process.

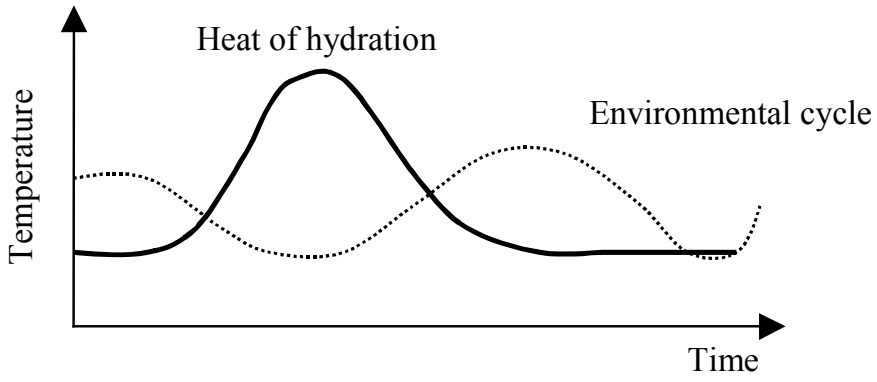


**Figure 8. Temperature in concrete pavement during hydration.**

### 3.3.2 Total Heat of Hydration of the Concrete

In addition to the kinetics of hydration, the total heat of hydration per cubic meter of concrete is an important factor in the prediction of the temperature rise in the pavement. Total heat of hydration is controlled by the content of cementitious materials (cement and fly ash) in the concrete. On the other hand, the capability of the heat to escape from the concrete to the atmosphere above and soil below is primarily controlled by the type and volume of aggregate (thermal diffusivity of the concrete).

### 3.3.3 Ultimate Strength of the Concrete

The tensile strength criterion for failure used in the HIPERPAV model indicates that the ultimate strength of the concrete is a critical parameter in the analysis. It is primarily controlled by the water-to-cement mass ratio and partly by the cementitious materials content and the angularity of the coarse aggregate (round gravel versus crushed granite).

### 3.3.4 Ultimate Thermo-Elastic Properties of the Concrete

Volume changes due to drying and vertical temperature gradients (warping and curling) create greater stresses when the concrete is stiffer. The thermo-elastic properties of the concrete (Young's modulus, coefficient of thermal expansion) depend on the type and the amount of aggregate used (stiff granite compared to soft gravel).

Water content was not selected as a variable for this because HIPERPAV does not directly take into account the drying shrinkage caused by the diffusion of water through the concrete. Instead, the drying shrinkage is directly correlated to the type and content of cementitious materials. A preliminary analysis confirmed this statement.

## 3.4 Selection of Variables

Based on Caltrans practice in 2001 and recommendations from UC PRC research, two sets of the four mix design variables discussed in Section 3.3 were selected, as shown in Table 3.(*5, 7–11*)

**Table 3 Combinations of Properties of Concrete**

| **Key feature** | **Set 1** | **Set 2** |
|---|---|---|
| Kinetics of hydration | Type III cement (rapid) | Type II cement (slow) |
| Thermo-elastic properties | Gravel coarse aggregate (soft) | Granite coarse aggregate (stiff) |
| Total heat of hydration | Less fly ash (0 or 15%) | More fly ash (25%) |
| Ultimate strength (Center point beam strength) | Lower strength (3.8 MPa/550 psi at 10 days for Type II concrete, 2.8 MPa/400 psi at 12 hours for Type III concrete) | Higher strength (4.5 MPa/650 psi at 10 days for Type II concrete, 3.1 MPa/450 psi at 12 hours for Type III concrete) |

Type III cement was not typical of Caltrans practice in 2001, but its inclusion in the mix design variables considered enables the evaluation of a wide range of kinetics. In addition, Type III cement is expected to play a more prominent role in Caltrans practice in the future. Aggregates normally used in California fall into the range of properties of gravel and granite.

Regarding the heat of hydration, it was decided to study the effect of fly ash since it is a material with a great potential for use in California, and Caltrans is increasingly using this material. Finally, the relatively low ultimate strength was based on Caltrans specifications in 2001, whereas the higher strength corresponds to research recommendations for somewhat greater strengths.(*7*)

The final experiment design includes 16 concrete mixes, as shown in Table 4. Mix design parameters were largely divided into two main groups according to the cement type: Type I/II and Type III. Both cement type groups had balanced factor levels for the other variables (i.e., aggregate type, strength gain, and Type F fly ash content). The values in each factor are, however, different for cement type in order to obtain realistic mix designs. The Type III cement concretes have higher 28-day compressive strengths than Type II cement concretes per the high early-age strength requirement for Type III cement concrete.

**Table 4 Combinations of Mix Design Parameters**

| Code | Cement Type | Aggregate Type | Fly ash Content | Strength Gain |
|---|---|---|---|---|
| M1 | Type (I/II) | Gravel | 15% | 3.8 MPa (550 psi) at10 days |
| M2 | | | | 4.5 MPa (650 psi) at 10 days |
| M3 | | | 25% | 3.8 MPa (550psi) at 10 days |
| M4 | | | | 4.5 MPa (650psi) at 10 days |
| M5 | | Granite | 15% | 3.8 MPa (550psi) at 10 days |
| M6 | | | | 4.5 MPa (650psi) at 10 days |
| M7 | | | 25% | 3.8 MPa (550psi) at 10 days |
| M8 | | | | 4.5 MPa (650psi) at 10 days |
| M9 | Type (III) | Gravel | 0% | 2.8 MPa (400psi) at 12 hours |
| M10 | | | | 3.1 MPa (450psi) at 12 hours |
| M11 | | | 25% | 2.8 MPa (400psi) at 12 hours |
| M12 | | | | 3.1 MPa (450psi) at 12 hours |
| M13 | | Granite | 0% | 2.8 MPa (400psi) at 12 hours |
| M14 | | | | 3.1 MPa (450psi) at 12 hours |
| M15 | | | 25% | 2.8 MPa (400psi) at 12 hours |
| M16 | | | | 3.1 MPa (450psi) at 12 hours |

The mix designs without fly ash were developed following the ACI 211.1-91 procedure for "Normal, Heavy Weight, and Mass Concrete," while the concretes with fly ash were designed by using the ACI 211.4R93 procedure for "High Strength Concrete with Ordinary Portland Cement and Fly Ash." The resulting mix designs were in some cases adapted to meet the following Caltrans specifications:

- minimum cementitious material requirement of 300 kg/m$^3$,
- water content less than 180 kg/m$^3$ plus 20kg for each 100kg of cement over 325kg/m$^3$).

Type F fly ash with low reactivity was chosen for the purpose of alkali-silica reaction prevention. The 28-day compressive strength ( $f'c$ ) used in the ACI mix design procedure was interpolated from the required strength at 10 days or 12 hours based on kinetics curves from Neville's book *Properties of Concrete* (*12*). The center point beam strength and the elastic modulus of concrete *E* were estimated using the following relationships in units of megapascals (MPa):

$$f_t \text{ centerpoint} = \frac{f_t \text{ thirdpoint}}{0.65}$$

$$f_t \text{thirdpoint} = 0.3 f'c^{2/3}$$

$$E = 4.73 f'c^{0.5}$$

Note that HIPERPAV does not permit input of beam strengths, which is the test Caltrans uses to test and specify pavement mixes.

Water reducer and superplasticizer agents have been added for low water-to-cement ratio high strength concretes.

## 3.5 Environmental Variables

The environmental variables were contained in two factors: region and season. Each of these two factors contains weather data such as maximum and minimum temperature, maximum and minimum humidity, average wind speed, and cloud cover data. Three climate regions and representative weather stations for each region were included in the experiment:

- Daggett, representing the Desert region,
- Los Angeles, representing the South Coast region, and
- San Francisco, representing the Bay Area region.

The weather data were obtained from the National Climate Data Center Website (*13*) and included the 10- year period 1990–2000. For the Season variable, the factors are February, May, and September. All the data and the code are shown in Table 5.

## 3.6 Construction Variables

The last category of variables is the construction variables. Construction variables are divided into four factors:

- curing method,
- construction start time,
- time to application of curing method
- time to saw cutting of joints

**Table 5 Combinations of Environmental Parameters**

| Code* | Region | Season | Max. Temp. (°C) | Min. Temp. (°C) | Max. Humidity (%) | Min. Humidity (%) | Cloud Cover | Avg. Wind Speed (km/h) |
|---|---|---|---|---|---|---|---|---|
| E1 | South Coast (Los Angeles) | February | 18.7 (65.6 °F) | 10.5 (50.9 °F) | 89.7 | 53.2 | Partly cloudy | 14.4 (8.9 MPH) |
| E2 | South Coast (Los Angeles) | May | 20.9 (69.7 °F) | 14.2 (57.5 °F) | 90.4 | 61.0 | Partly cloudy | 13.3 (8.2 MPH) |
| E3 | South Coast (Los Angeles) | September | 24.7 (76.5 °F) | 17.6 (63.6 °F) | 90.7 | 59.3 | Sunny | 12.2 (7.6 MPH) |
| E1 | Desert (Daggett) | February | 19.1 (66.3 °F) | 5.3 (41.5 °F) | 72.9 | 28.8 | Sunny | 15.1 (9.4 MPH) |
| E2 | Desert (Daggett) | May | 31.6 (88.8 °F) | 15.1 (59.2 °F) | 54.3 | 15.6 | Sunny | 22.9 (14.2 MPH) |
| E3 | Desert (Daggett) | September | 35.8 (96.4 °F) | 18.7 (65.7 °F) | 46.8 | 14.9 | Sunny | 15.8 (9.8 MPH) |
| E1 | Bay Area (San Francisco) | February | 15.3 (59.6 °F) | 8.3 (47.0 °F) | 94.7 | 63.0 | Cloudy | 13.9 (8.6 MPH) |
| E2 | Bay Area (San Francisco) | May | 19.6 (67.3 °F) | 11.1 (51.9 °F) | 89.7 | 54.3 | Partly cloudy | 21.9 (13.6 MPH) |
| E3 | Bay Area (San Francisco) | September | 22.9 (73.2°F) | 13.1 (55.6 °F) | 92.6 | 54.2 | Sunny | 17.6 (11.0 MPH) |

* Note: For the California case overview analyses (Figures 12 and 22), the environmental parameters had to be summarized because of the limits of the customized (spreadsheet-based) HIPERPAV software. The environmental parameters were averaged into three seasonal groups (E1, E2, and E3), representing February, May, and September for the entire state, respectively. That is, E1 is the average of February for all three climate regions (South Coast, Desert, and Bay Area). This decision was made based on the preliminary sensitivity analysis for the input categories, which showed that the environmental parameters have the least effect on the HIPERPAV results compared to the other categories (i.e., design, mix design, and construction).

Among the seven curing method types available in HIPERPAV, three types were chosen: none, double coat liquid curing compound, and cotton mats or burlap. For the construction starting times, 6 A.M., 2 P.M., and 10 P.M. were selected. Zeros for curing application and saw cutting time mean that a curing method was applied and joints saw cut at the correct times with no delay. The other values for these variables indicated that curing method and saw cutting were delayed or never performed. PCC mixture temperatures were selected after consideration of the construction start time and the standard temperature limit used by Caltrans, and reflect the fact that the mixture temperature can be changed physically. For the 6 A.M. start time, 10°C (50°F)

was used; for the 2 P.M. start time, 30°C (86°F) was used; and for the 10 P.M. start, 20°C (68°F) was used.

The subbase temperature was assumed to be controlled by the air temperature at the time of concrete placement. The average of the minimum temperature in each month was used for the 6 A.M. construction start, maximum average for the 2 P.M. start, and total average for 10 P.M. start. With this calculation, the subbase temperature is discrete for the different regions, as shown in Table 5.

Table 6 shows the complete construction variables for the case of Daggett.

### 3.7 Batch Mode of Operation for HIPERPAV

The experiment design factorial described in this chapter results in a total of 93,312 cases (the product of 18 design variables, 16 mixes, 9 environmental conditions, and 36 construction variables). After a pilot study on a small sample of the experiment, it was estimated that it would take graduate students 9 person-months to complete this task using the single case by single case operating mode of HIPERPAV. To obtain a more efficient method of generating the results, an arrangement was made with the developers of HIPERPAV to create a customized batch mode version of the program.

The batch mode is a Microsoft® Excel based program, which is modified to give flexibility in the input system. All possible combinations of input variables can be input at once in this version, and it produces the output on one sheet. Figure 9 shows an output sheet of the batch mode HIPERPAV.

After generating the results using the batch mode HIPERPAV, the results were exported to the software SPLUS, a statistical modeling and analysis solution, for sensitivity analysis.

**Table 6 Combinations of Construction Parameters for Daggett (Desert Climate Region)**

| Code | Curing Method | Construction Start Time | Cure Time Delay (hr) | Sawcut Time Delay (hr) | PCC Mix Temperature °C (°F) | Subbase Temp.(°C) |
|---|---|---|---|---|---|---|
| C1 | None | 6 A.M. | 0 | 0 | 10 (50) | 13 (56) |
| C2 | None | 6 A.M. | 0 | 24 | 10 (50) | 13 (56) |
| C3 | None | 6 A.M. | 6 | 0 | 10 (50) | 13 (56) |
| C4 | None | 6 A.M. | 6 | 24 | 10 (50) | 13 (56) |
| C5 | None | 2 P.M. | 0 | 0 | 30 (86) | 29 (84) |
| C6 | None | 2 P.M. | 0 | 24 | 30 (86) | 29 (84) |
| C7 | None | 2 P.M. | 6 | 0 | 30 (86) | 29 (84) |
| C8 | None | 2 P.M. | 6 | 24 | 30 (86) | 29 (84) |
| C9 | None | 10 P.M. | 0 | 0 | 20 (68) | 20.9 (69.7°F) |
| C10 | None | 10 P.M | 0 | 24 | 20 (68) | 20.9 (69.7°F) |
| C11 | None | 10 P.M | 6 | 0 | 20 (68) | 20.9 (69.7°F) |
| C12 | None | 10 P.M | 6 | 24 | 20 (68) | 20.9 (69.7°F) |
| C13 | Double Coat Liquid Curing Compound | 6 A.M. | 0 | 0 | 10 (50) | 13.1 (55.5°F) |
| C14 | Double Coat Liquid Curing Compound | 6 A.M. | 0 | 24 | 10 (50) | 13.1 (55.5°F) |
| C15 | Double Coat Liquid Curing Compound | 6 A.M. | 6 | 0 | 10 (50) | 13.1 (55.5°F) |
| C16 | Double Coat Liquid Curing Compound | 6 A.M. | 6 | 24 | 10 (50) | 13.1 (55.5°F) |
| C17 | Double Coat Liquid Curing Compound | 2 P.M. | 0 | 0 | 30 (86) | 28.8 (83.9°F) |
| C18 | Double Coat Liquid Curing Compound | 2 P.M. | 0 | 24 | 30 (86) | 28.8 (83.9°F) |
| C19 | Double Coat Liquid Curing Compound | 2 P.M. | 6 | 0 | 30 (86) | 28.8 (83.9°F) |
| C20 | Double Coat Liquid Curing Compound | 2 P.M. | 6 | 24 | 30 (86) | 28.8 (83.9°F) |
| C21 | Double Coat Liquid Curing Compound | 10 P.M | 0 | 0 | 20 (68) | 20.9 (69.7°F) |
| C22 | Double Coat Liquid Curing Compound | 10 P.M | 0 | 24 | 20 (68) | 20.9 (69.7°F) |
| C23 | Double Coat Liquid Curing Compound | 10 P.M | 6 | 0 | 20 (68) | 20.9 (69.7°F) |
| C24 | Double Coat Liquid Curing Compound | 10 P.M | 6 | 24 | 20 (68) | 20.9 (69.7°F) |
| C25 | Burlap | 6 A.M. | 0 | 0 | 10 (50) | 13.1 (55.5°F) |
| C26 | Burlap | 6 A.M. | 0 | 24 | 10 (50) | 13.1 (55.5°F) |
| C27 | Burlap | 6 A.M. | 6 | 0 | 10 (50) | 13.1 (55.5°F) |
| C28 | Burlap | 6 A.M. | 6 | 24 | 10 (50) | 13.1 (55.5°F) |
| C29 | Burlap | 2 P.M. | 0 | 0 | 30 (86) | 28.8 (83.9°F) |
| C30 | Burlap | 2 P.M. | 0 | 24 | 30 (86) | 28.8 (83.9°F) |
| C31 | Burlap | 2 P.M. | 6 | 0 | 30 (86) | 28.8 (83.9°F) |
| C32 | Burlap | 2 P.M. | 6 | 24 | 30 (86) | 28.8 (83.9°F) |
| C33 | Burlap | 10 P.M | 0 | 0 | 20 (68) | 20.9 (69.7°F) |
| C34 | Burlap | 10 P.M | 0 | 24 | 20 (68) | 20.9 (69.7°F) |
| C35 | Burlap | 10 P.M | 6 | 0 | 20 (68) | 20.9 (69.7°F) |
| C36 | Burlap | 10 P.M | 6 | 24 | 20 (68) | 20.9 (69.7°F) |

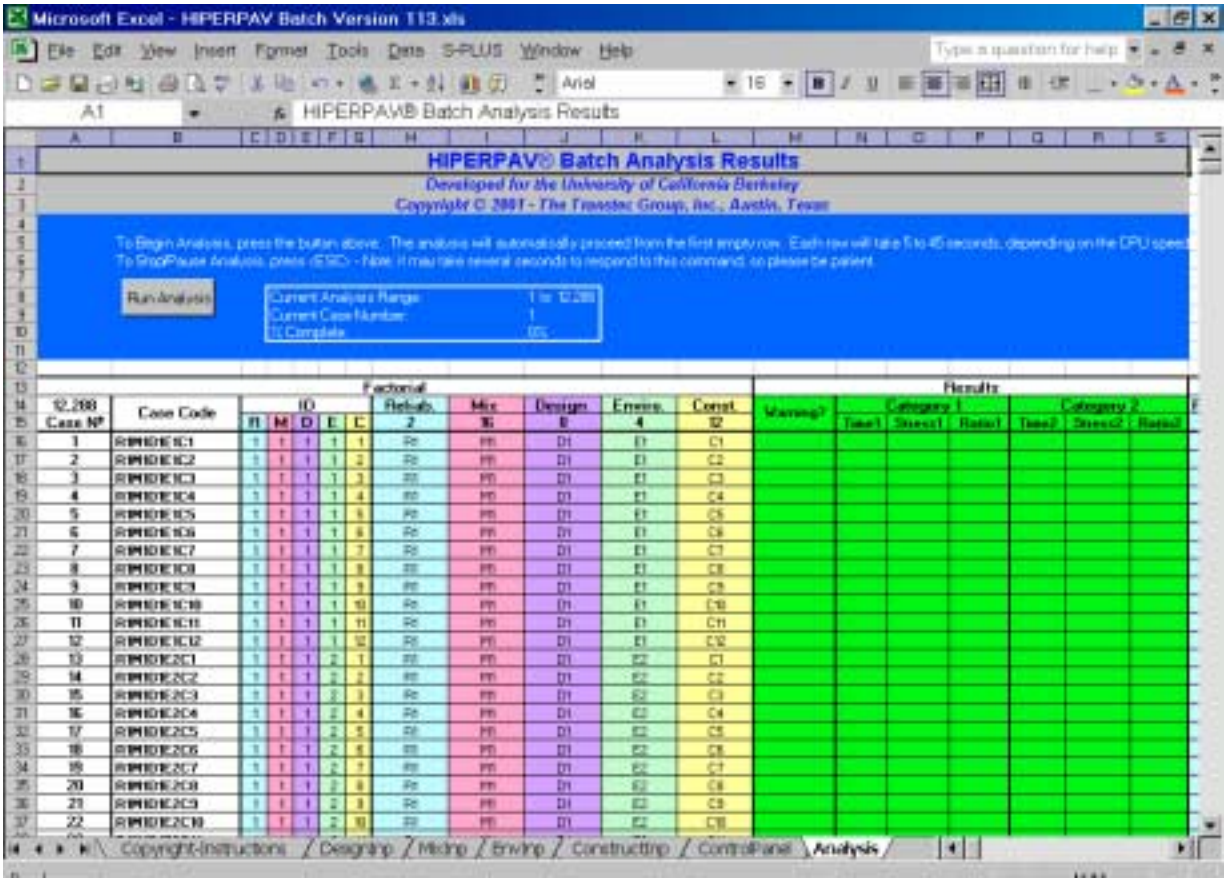


**Figure 9. Output screen of the batch mode HIPERPAV**

## 4.0 RESULTS AND ANALYSIS

For this study, two statistical approaches were used to evaluate the results from HIPERPAV, which are referred to in this report as *Ratio mode* and *Failure mode*. HIPERPAV currently provides results only in the Failure mode, although the user can perform the calculation to obtain a Ratio mode result.

Failure mode is binary and indicates only whether the predicted stress was greater than or equal to the predicted strength, in which case cracking is predicted, or that the stress was less than the strength, in which case no cracking is predicted. For the results in this report, the cracking cases were assigned a value of 1 while the non-cracking cases are assigned a value of 0. Therefore, the probability of failure is the number of cases for which cracking is predicted divided by the total number of cases.

In Ratio mode analysis, the dependent variable from HIPERPAV is the ratio of the predicted strength divided by the predicted stress, referred to as the *strength-to-stress ratio* in this report. This variable provides an indication of the risk of cracking, with increasing values indicating reduced risk of cracking. The average risk of cracking for a given factor level in the experiment can be evaluated from the average of the strength-to-stress ratios for that factor level.

Rules were developed to select the strength-to-stress ratio for statistical analysis from the cycles of stress and strength estimated by HIPERPAV in the first 72 hours after placement of the concrete. If at any time in the 72-hour period HIPERPAV predicted a strength-to-stress ratio of 1.0 or less, indicating failure, the strength-to-stress ratio at the peak of the cycle in which failure occurred was used. If the strength-to-stress ratio was never less than 1.0, then the smallest strength-to-stress ratio (highest risk of cracking) predicted by HIPERPAV in the 72-hour period was selected. The graphical explanation of the Failure and Ratio modes is shown in Figure 10.

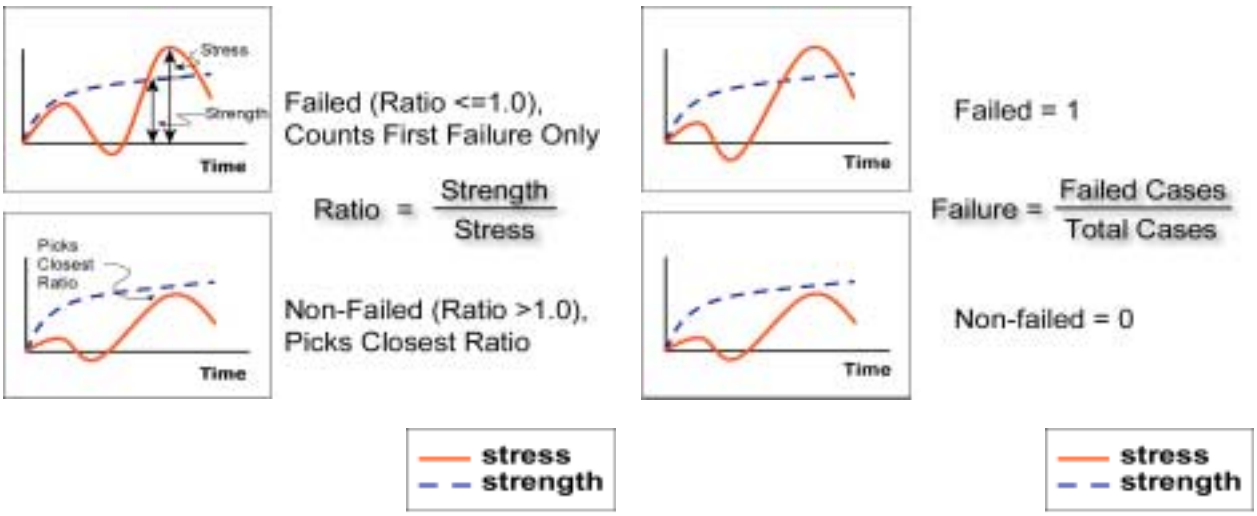


**Figure 10a. Ratio Mode.** **Figure 10b. Failure Mode.**

**Figure 10. The dependent parameters in Ratio mode and Failure mode.**

A great deal of information is lost if the results of this study are evaluated in the Failure mode, since the relative risk of failure is not considered, only whether failure was predicted. For this reason, most of the analysis included in this chapter uses the Ratio mode results.

## 4.1 Reading the Sensitivity Figures

Figure 11 shows an example of a sensitivity analysis figure. The horizontal line in each figure is the total average value for all cases related with the parameters considered in the given figure (Mean of Category). Since the parameters shown in each figure cover all the cases, the total average value is identical in all the figures except the figures for the two different cement types (each cement type represents half of the total cases). The short horizontal bar shows the mean value for the given parameter (Mean of Parameter). The vertical line represents the varying range of the strength-to-stress ratio as the parameters change. The wider the range for a

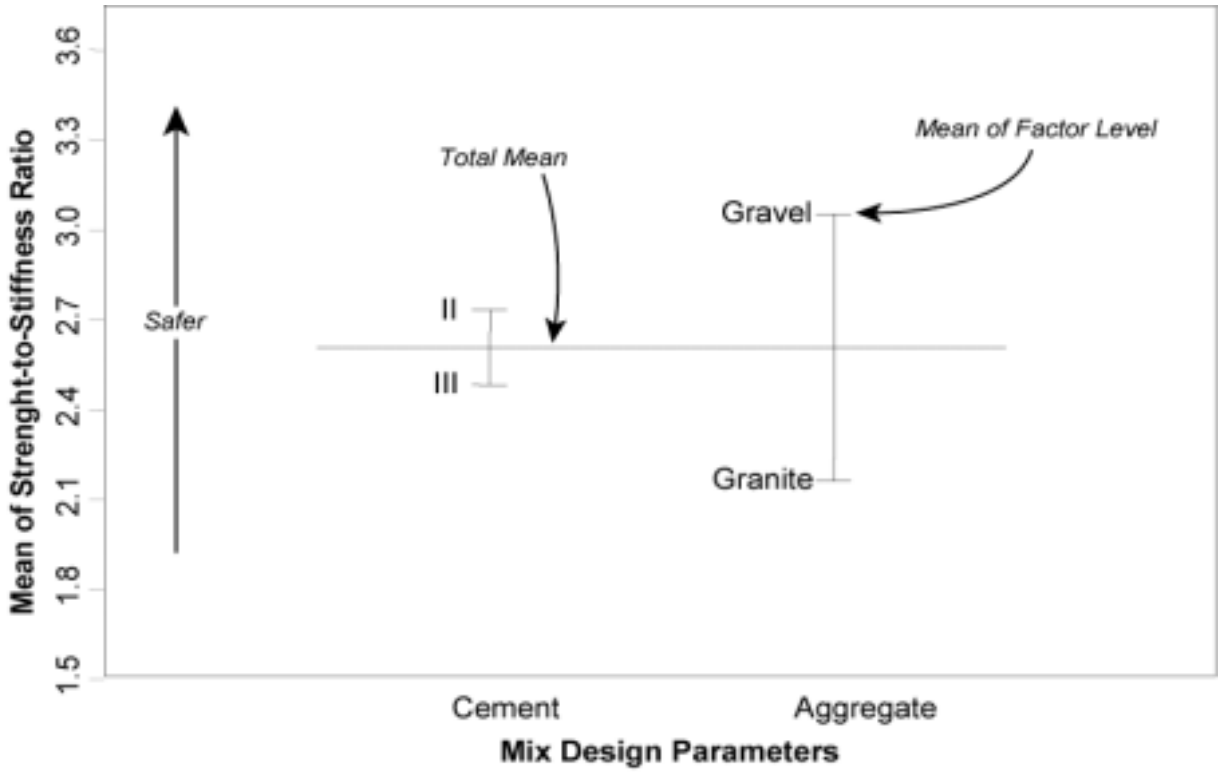


**Figure 11. A schematic showing how to read the sensitivity figures.**

given parameter, the more sensitive the strength-to-stress ratio to that parameter for the factor levels considered. A narrower range means that that the strength-to-stress ratio is less sensitive to that parameter for the factor levels considered. A higher strength-to-stress ratio for a given option means that the option has a lower risk of early-age cracking. The figures within each mode of analysis (i.e., Ratio or Failure) all have the same scale, allowing direct comparison among cases within a mode, but not between modes.

## 4.2 Overall Parametric Sensitivity

Figure 12 shows the relative strength-to-stress ratio sensitivity to the variables across all cases. As shown in the figure, construction parameters have the greatest effect on the strength-

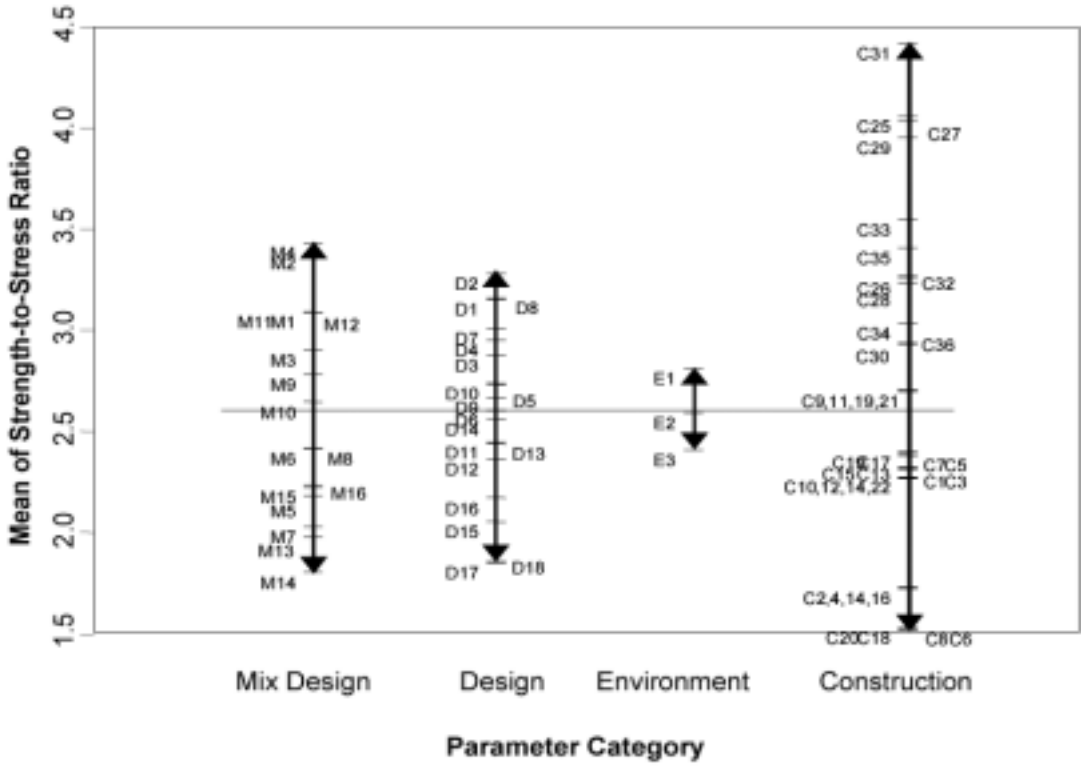


**Figure 12. Relative sensitivity of the strength-to-stiffness ratio (Ratio mode analysis) to the four parameter categories, overall California case.**

to-stress ratio while the environment parameters have the least (see Section 3.6). The case numbers shown in Figure 12 are defined in Tables 2–6.

Table 7 summarizes the effect of each group of parameters in each region. Note that for all three climate regions, the results are most sensitive to construction parameters. The second most influential group of parameters is mix design, followed by the design and environment parameters.

Comparison of the total range of strength-to-stress ratios obtained for the three climate regions across all the other variables in the experiment design shows an increase in sensitivity to the input parameters moving from the Desert to Los Angeles to the Bay Area. The range of

**Table 7 Relative Sensitivity to Parameter Types by Climate Region**

| Climate Region | Parameter | Maximum Strength-To-Stress Ratio | Minimum Strength-To-Stress Ratio | Range | Relative Sensitivity (%)* |
|---|---|---|---|---|---|
| Desert (Daggett) | Mix Design | 2.6 | 1.6 | 1 | 21.1 |
| | Design | 2.5 | 1.55 | 0.95 | 20.0 |
| | Environment | 2.2 | 2 | 0.2 | 4.2 |
| | Construction | 3.8 | 1.2 | 2.6 | 54.7 |
| South Coast (Los Angeles) | Mix Design | 3.9 | 1.9 | 2 | 30.3 |
| | Design | 3.5 | 2 | 1.5 | 22.7 |
| | Environment | 3.1 | 2.7 | 0.4 | 6.1 |
| | Construction | 4.5 | 1.8 | 2.7 | 40.9 |
| Bay Area (San Francisco) | Mix Design | 4 | 1.9 | 2.1 | 23.9 |
| | Design | 3.8 | 1.9 | 1.9 | 21.6 |
| | Environment | 3.7 | 1.3 | 2.4 | 14.8 |
| | Construction | 5 | 1.5 | 2.0 | 39.8 |

* In Table 7, relative sensitivity is calculated as the range of a given parameter divided by the sum of the ranges for the climate region. For example, the relative sensitivity of mix design in Daggett is 21.1 = 1/ (1+0.95+.2+2.6).

results for Daggett is 39 percent less than the range for Los Angeles and the range of results for Los Angeles is 33 percent less than the range for San Francisco. At the same time, the average strength-to-stress ratio is greater in San Francisco than in Los Angeles, and greater in Los Angeles than in Daggett, indicating that the risk of early-age cracking is greater in the desert than in the coastal areas.

The increase in sensitivity to the input parameters in the Bay Area compared to the other regions is partly due to the broader range of environmental conditions occurring across the three seasons in the Bay Area in terms of wind speed and insulation, and the fact that the effects of the temperature and humidity ranges do not seem to be very significant. These results may also be explained by the fact that the temperature increase from the heat of hydration of cement and from external conditions (insulation) is equally important in the Bay Area. In contrast, in the Desert

region (Daggett) the effect of external temperature rise from the hot environment surpasses the differences in heat of hydration for the different cements and mixes.

### 4.2.1 Effect of Construction Parameters

Among the construction parameters, the curing method and the time to saw cutting of joints are especially critical for minimizing early-age cracking, as shown in Figure 13.

#### *4.2.1.1 Curing treatment*

The high variability between burlap curing and no curing is mainly due to the insulating effect of the burlap. The burlap reduces the solar radiation (lower absorption coefficient) and the temperature difference between the top and the bottom of the pavement by thermal insulation.

As expected, HIPERPAV does not predict any improvement due to a double coat of liquid curing compound because the program does not model the diffusion process of water. The double coat of liquid curing compound will not change the solar radiation absorption properties of the concrete surface, but it will greatly reduce the drying rate at the concrete surface. Therefore, it would be expected that a double coat of liquid curing compound would significantly reduce early-age cracking even though HIPERPAV does not indicate that result. The high sensitivity to the time to saw cutting of joints is expected because early cracking usually occurs during the first 24 hours of hydration if sawing is not performed.

#### *4.2.1.2 Construction start time*

The construction start time, which because of the temperature at a given time of the day will affect the initial time of hydration, shows a small effect on the cracking phenomena. The 6 A.M. (6 hour) and 2 P.M. (14 hour) start times have a greater risk of early-age cracking than 10

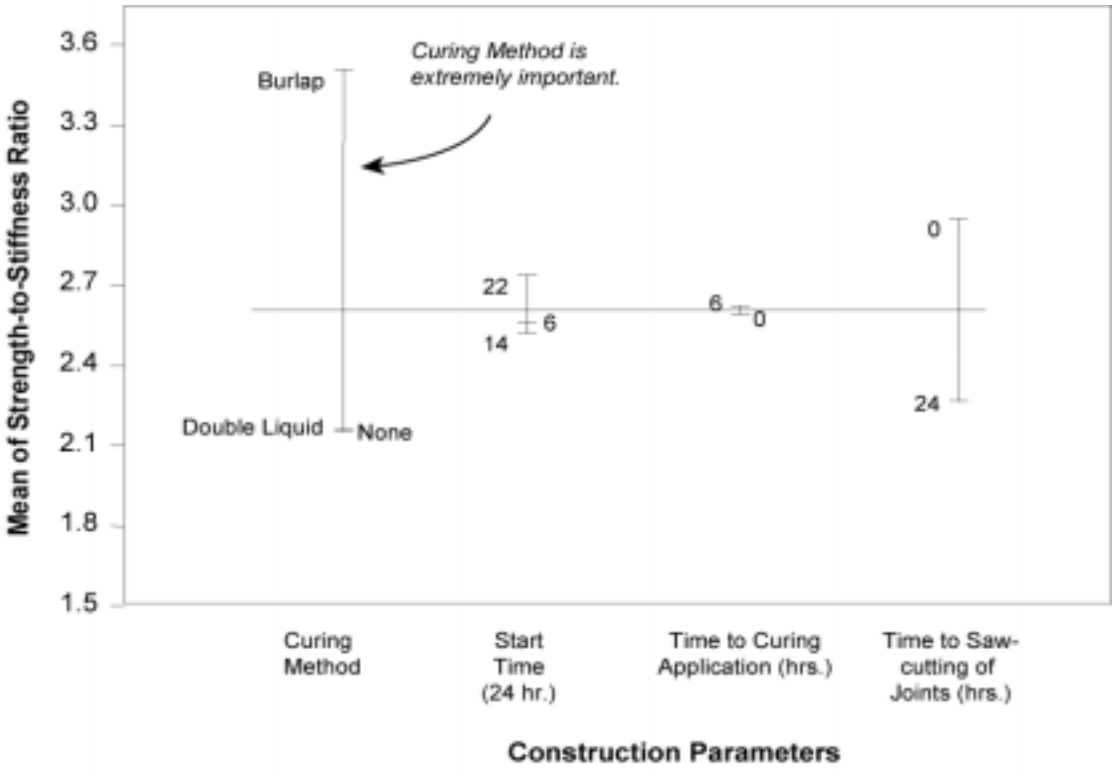


**Figure 13. Effects of construction parameters on strength-to-stiffness ratio (Ratio mode analysis).**

P.M. (22 hour). This effect can be explained by the initial temperature and the kinetics of hydration in all situations, as shown in Table 8. A 10 P.M. start time results in a low initial temperature of the concrete and a low temperature during the rapid hardening process (usually occurring between 4 and 8 hours after initial hydration). A 6 A.M. start time will cause a low initial temperature of the concrete, but a high temperature during the rapid hardening process, which will exacerbate the temperature increase due to hydration heat. A 2 P.M. start time will cause a high initial temperature of the fresh concrete, but a low temperature during the rapid hardening process, which will increase the stresses in the cooling process.

**Table 8 Effect of Construction Start Time and Temperature**

| Construction Start Time | Initial External Temperature (Air and Subbase) | Air Temperature When Heat Release From Hydration Peaks (After 6 Hours) |
|---|---|---|
| 6 A.M. | Low | High |
| 2 P.M. | High | Low |
| 10 P.M. | Low | Low |

*4.2.1.3 Time of placement of curing treatment*

HIPERPAV indicates that the timing of the placement of a curing treatment has a minor influence on early-age cracking, regardless of whether the treatment is placed immediately after placing the concrete or 6 hours after placing the concrete because the insulation effect is not affected by the time at which burlap is applied.

However, it is likely that HIPERPAV would predict a larger effect of the time to placement of a curing treatment if the diffusion of water were taken into account in the model. A water diffusion model would affect HIPERPAV prediction because most bleeding occurs within the first hours of hydration, and it is critical to apply the curing compound early enough to mitigate bleeding water on the surface of the concrete.

4.2.2 Effects of Mix Design Parameters

Cement type, aggregate type, fly ash content, and strength gain are all determined in the mix design. Because fly ash content and strength gain vary according to the cement type, the effect of cement type and aggregate type on results are presented first (Figure 14). The effects of the other mix design variables are separated and presented by the cement type.

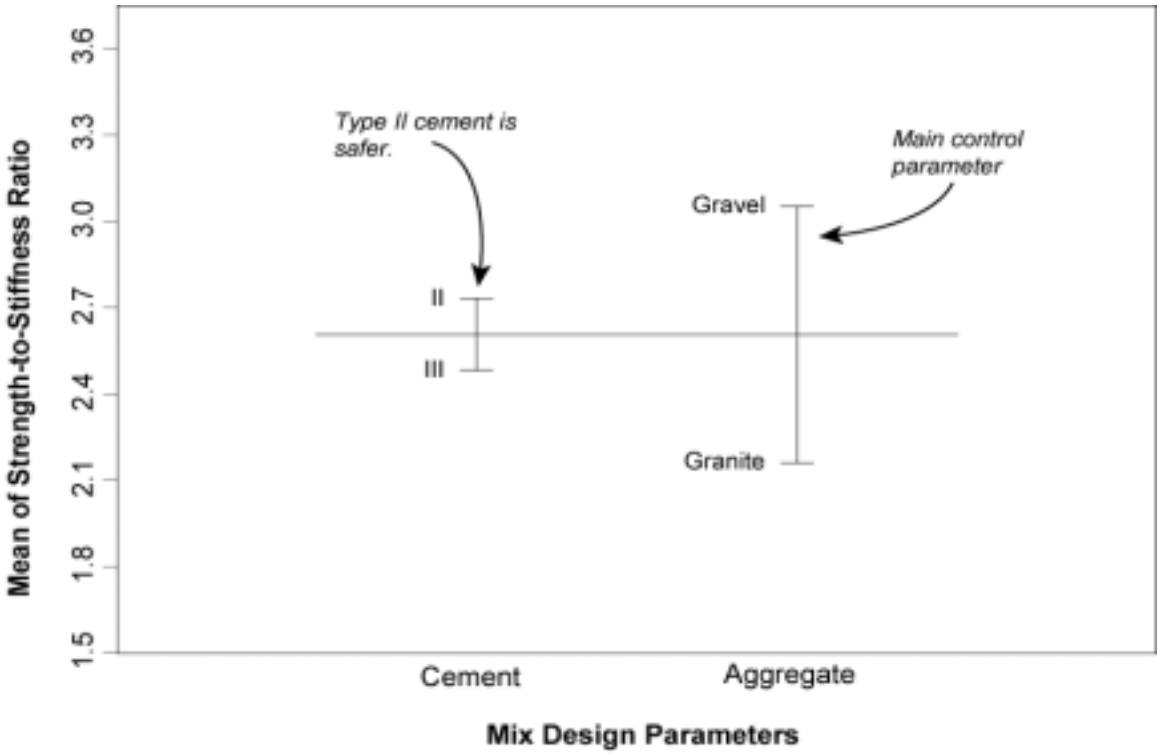


**Figure 14. Effect of mix design parameters on strength-to-stiffness ratio (Ratio mode analysis).**

According to HIPERPAV, among cement type and aggregate type, the effect of aggregate type has the greatest impact on the risk of early-age cracking. This effect can be explained by the difference in the coefficient of thermal expansion (CTE) and in the stiffness of the two aggregate types.

The effect of angularity is not taken into account in HIPERPAV. Gravel aggregates are softer but have a higher CTE compared to granite aggregates. The fact that HIPERPAV predicts that gravel aggregates significantly reduce the risk of early-age cracking compared to granite coarse aggregates shows that the elastic properties are more important than the thermal properties. In other words, the effect of stress generation from the strain is more important than the strain generation itself.

The strength and the amount of fly ash both affect early-age cracking. The replacement of cement by fly ash reduces the heat generation during hydration, thereby reducing the risk of

early-age cracking. If the two types of cement (Figure 15 Type II; Figure 16 Type III) are considered separately, then the addition of fly ash will always decrease the risk of cracking. It is important to note that the effect of fly ash is probably greater than that predicted by HIPERPAV because the software does not account for the diffusion of water through the concrete (lower permeability and bleeding rate for fly ash concretes).

Concerning the effect of the tensile strength, the two types of cement need to be considered separately:

- Concrete mixes with slower hydrating cement (Type II), which are required to reach their specified strength at 10 days, produce compressive strengths at 28 days of 30 MPa (4400 psi) to 40 MPa (5800 psi).
- Concrete mixes with faster hydrating cements (Type III) also usually have greater ultimate strengths, with compressive strength at 28 days of 48 MPa (7000 psi) to 83 MPa (12000 psi).

Overall, Type II concretes are more resistant to early-age cracking than Type III concretes, as can be seen by the difference in the mean strength-to-stress ratios between Figures 15 and 16. These results can be explained by the following causes:

a. **Heat generation:** Type II cement concretes have a lower rate of heat generation than Type III cement concretes.
b. **Development of elastic properties:** Type II cement concretes have a lower elastic modulus than Type III cement concretes when they cool down and therefore generate less stress.
c. **Resistance to cracking:** The higher resistance to cracking (higher tensile strength) is overcome by the greater generation of stress in the case of Type III cement concretes.

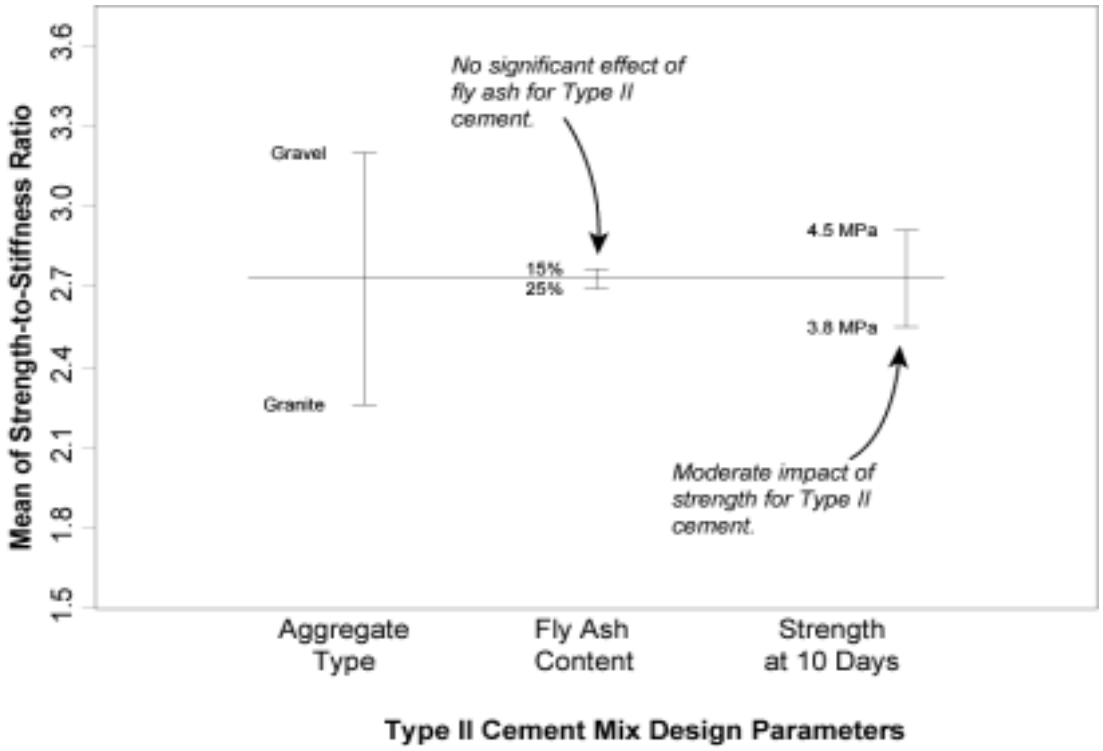


**Figure 15. Effects of Type II cement mix design parameters on strength-to-stiffness ratio (Ratio mode analysis) for overall California case.**

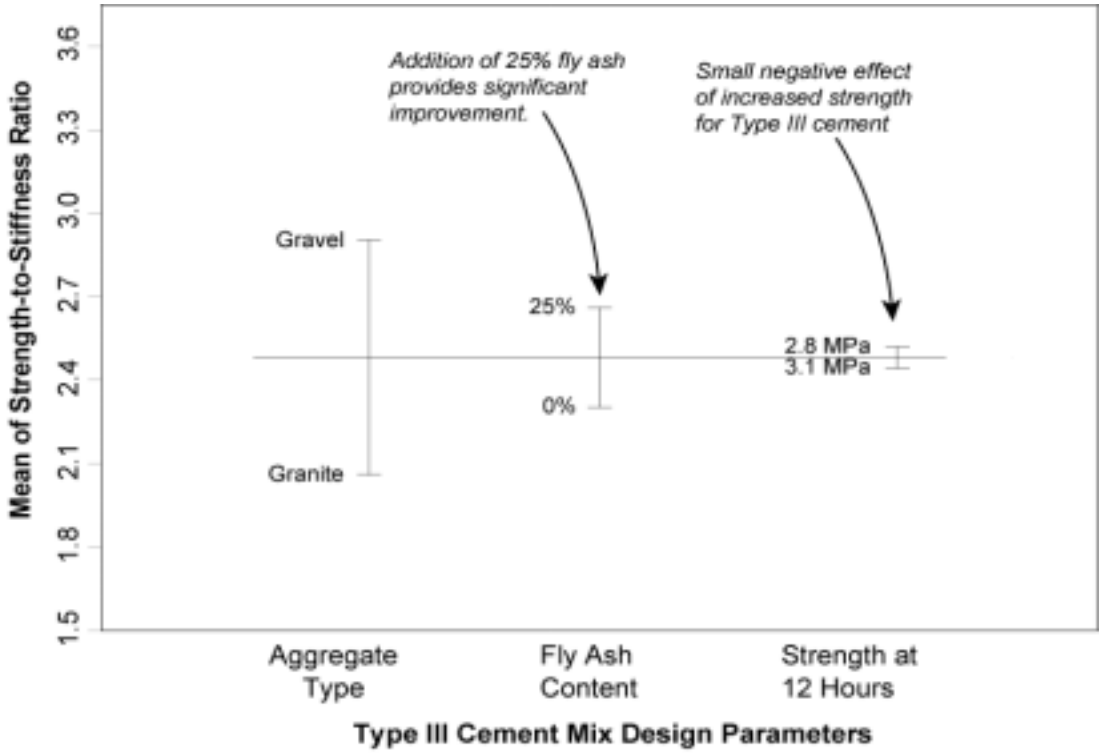


**Figure 16. Effects of Type III cement mix design parameters on strength-to-stiffness ratio (Ratio mode analysis) for overall California case.**

For the Type II concretes (3.8 MPa/550 psi and 4.5 MPa/650 psi tensile strength gain in 10 days), higher strength gives lower risk of cracking, as resistance to cracking becomes the only important factor.

In the case of Type III concretes (2.8 MPa/400 psi and 3.1 MPa/450 psi tensile strength in 12 hours), higher strength increases the risk of cracking as heat generation and development of elastic properties become the key factors.

Finally, it can be seen that the effect of the cement type on the risk of cracking is relatively small. On average over all regions, Type II concrete reduces the risk of early-age cracking. This effect is probably minimized due to the difference in the ultimate strength. Type III concretes have much higher 28-day strength than Type II concretes in order to meet their high early-age strength requirement. Since the heat of hydration is less of a factor than external conditions in hot regions, the faster kinetics of hydration of Type III concretes do not have much effect in the Desert and Central Valley. However, since their strengths at any given time are much higher than those of Type II cements, they are predicted to crack at higher stress levels (almost all the mechanical properties in HIPERPAV are based on 28-day compressive strength).

In summary, HIPERPAV confirms that the use of a softer coarse aggregate combined with the use of fly ash and slow cement (Type II) greatly reduces the overall risk of early-age cracking.

### 4.2.3 Effect of Design Parameters

The risk of cracking as predicted by HIPERPAV is particularly sensitive to subbase type and joint spacing, as shown in Figure 17. A cement stabilized base creates a condition of higher friction at the subbase/concrete pavement interface and higher risk of cracking compared to a smooth hot mix asphalt (HMA) concrete base. Similarly, a 5.7-m (19-ft.) joint spacing will

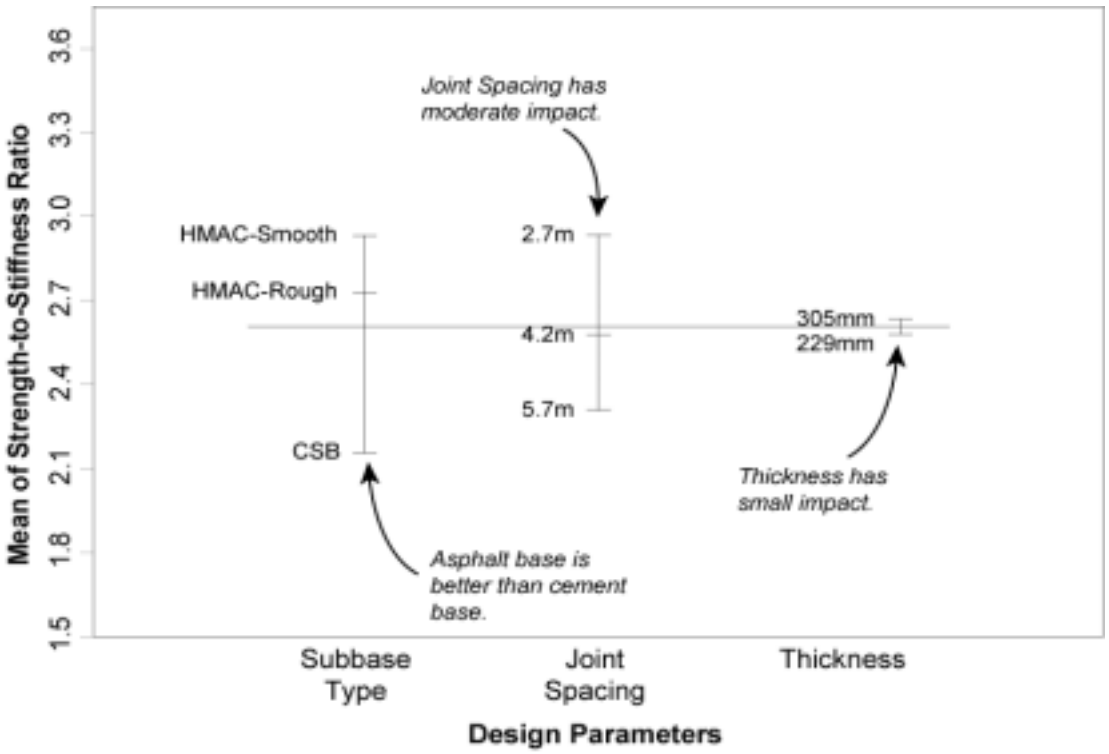


**Figure 17. Effect of pavement design parameters on strength-to-stiffness ratio (Ratio mode analysis) for overall California case.**

create more stresses than a 2.7-m (9-ft.) joint spacing because the accumulated drying strains and the curling stresses are higher. Thickness does not significantly affect the strength-to-stress ratio computed by HIPERPAV, primarily due to offsetting of the positive effect of the thickness on the structural behavior of the slab (lower stress) and the negative effect of higher temperature gradients and greater self-weight.

### 4.2.4 Effect of Environment Parameters

On average, for the three California climates analyzed, HIPERPAV indicates that the season in which concrete is placed has a weak effect on early-age cracking (Figure 18). The month of February poses less risk of early-age cracking than May, which is in turn safer than September. This difference can be explained by the harsher average conditions (greater solar

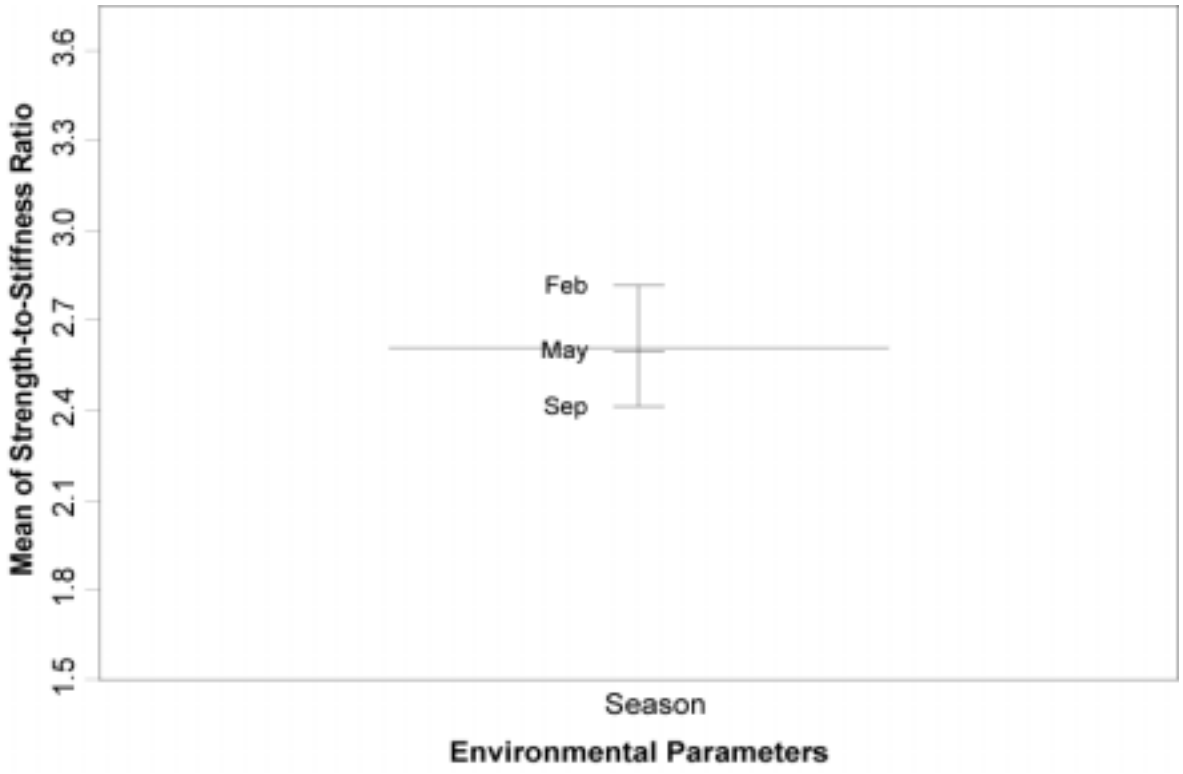


**Figure 18. Effect of environmental parameters on strength-to-stiffness ratio (Ratio mode analysis) for overall California case.**

radiation, more wind, higher temperature, and lower humidity) of September compared to May and February for the three regions.

### 4.3 Parametric Sensitivity Analysis by Climate Region

The results of the sensitivity analysis performed by climate region are similar to the overall sensitivity analysis results except for of the mix design parameters.

In the Desert region (Daggett), effects of hydration heat generation are outweighed by hot environmental conditions. For this reason, the risk of early-age cracking due to mix design parameters such as cement type and fly ash quantity is generally more sensitive in the South Coast (Los Angeles) and Bay Area (San Francisco) climate regions. However, the effect of

aggregate type, especially the coefficient of thermal expansion of the aggregate, is greater for the Desert region because of its interaction with the external conditions (solar radiation, temperature) in the desert area. Figures 19–21 show the sensitivities to mix parameters by region.

Note the overall greater risk (lower average strength-to-stress ratio) in the Desert region compared to the other regions in Figures 19–21.

For the Desert region (Daggett), Type III cement is shown to be less risky for early-age cracking than Type II cement. This seemingly contradictory result can be explained by the fact that the ultimate strength is the key factor in this case. Type III cements have much higher 28-day strengths than Type II cements. The heat of hydration is less of a key factor for Type III cements than the external environment on slab temperatures in hot regions, therefore the kinetics of hydration do not increase the risk of early-age cracking as much as the higher early strength

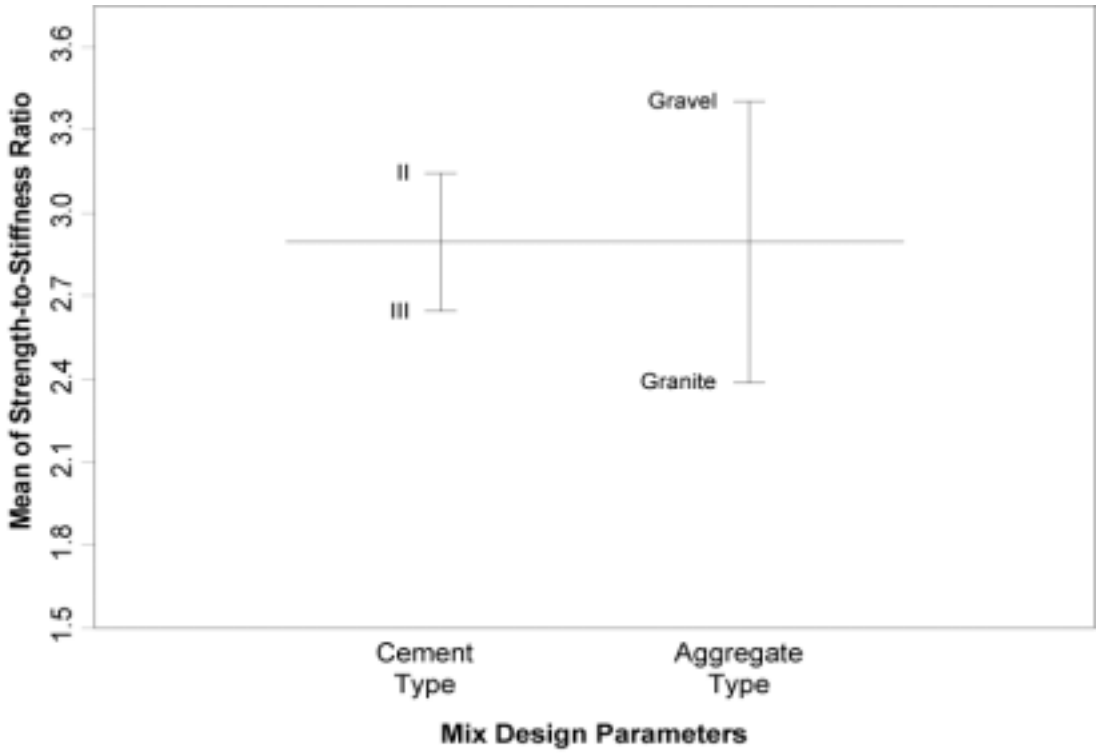


**Figure 19. Effect of mix design parameters on strength-to-stiffness ratio (Ratio mode analysis) for Bay Area region (San Francisco).**

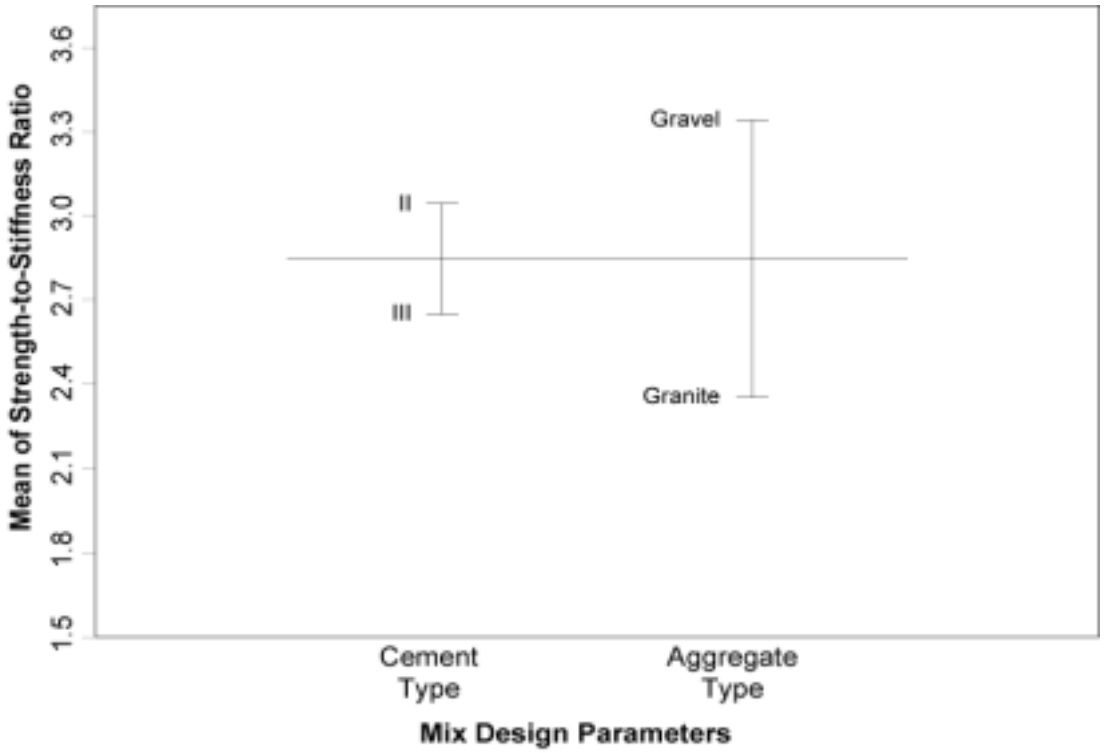


**Figure 20. Effect of mix design parameters on strength-to-stiffness ratio (Ratio mode analysis) for South Coast region (Los Angeles).**

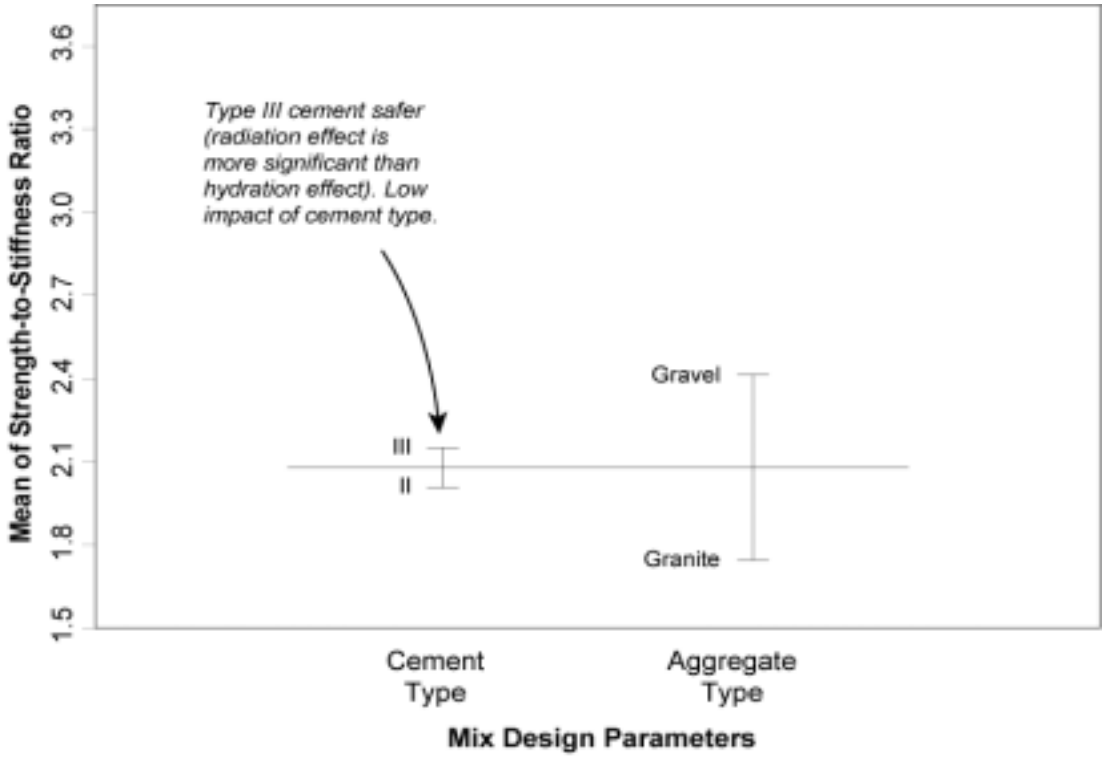


**Figure 21. Effect of mix design parameters on strength-to-stiffness ratio (Ratio mode analysis) for Desert region (Daggett).**

reduces this risk, compared to Type II cements. This is also shown by the effect of strength on the strength-to-stress ratio—higher strength will uniformly reduce the risk of early-age cracking.

In terms of the overall sensitivity to seasonal changes, the Bay Area region shows a higher sensitivity to seasonal variation, which is expected with that region's broader range of environmental conditions.

### 4.4 Failure Sensitivity Analysis

From a designer's viewpoint, Failure mode sensitivity analysis is more convenient because it simply reports failure or non-failure with a binary value (failure has a value of 1 while non-failure has a value of 0). However, a great deal of information is lost when HIPERPAV is used as a failure/non-failure prediction tool. The results of Failure mode analysis are also dependent on how the reliability value is set.

In the Ratio mode analysis, the results can be compared for reliability, with a greater value indicating increased safety, or more reliable resistance to early-age cracking. Note that a failed condition in Failure mode has a value of 1 while non-failure has a value of 0 (lower value is safer) while in Ratio mode, a higher value is safer.

As shown in Figure 22, the sensitivity analysis of the Failure mode for the overall California parameters follow the similar trends of the Ratio mode sensitivity except that the mix design parameters have the biggest impact, which possibly resulted from a bias of the binary values (0 or 1) (see Section 3.6).

For example, the results of the Failure mode analysis for mix design parameters for Type II cement (Figure 23) have the same trend as the results from the Ratio mode analysis (Figure 15). Because the optimal value is low for Failure mode analysis and high for Ratio mode analysis, the order of parameters in Failure mode analysis is different from that of Ratio mode

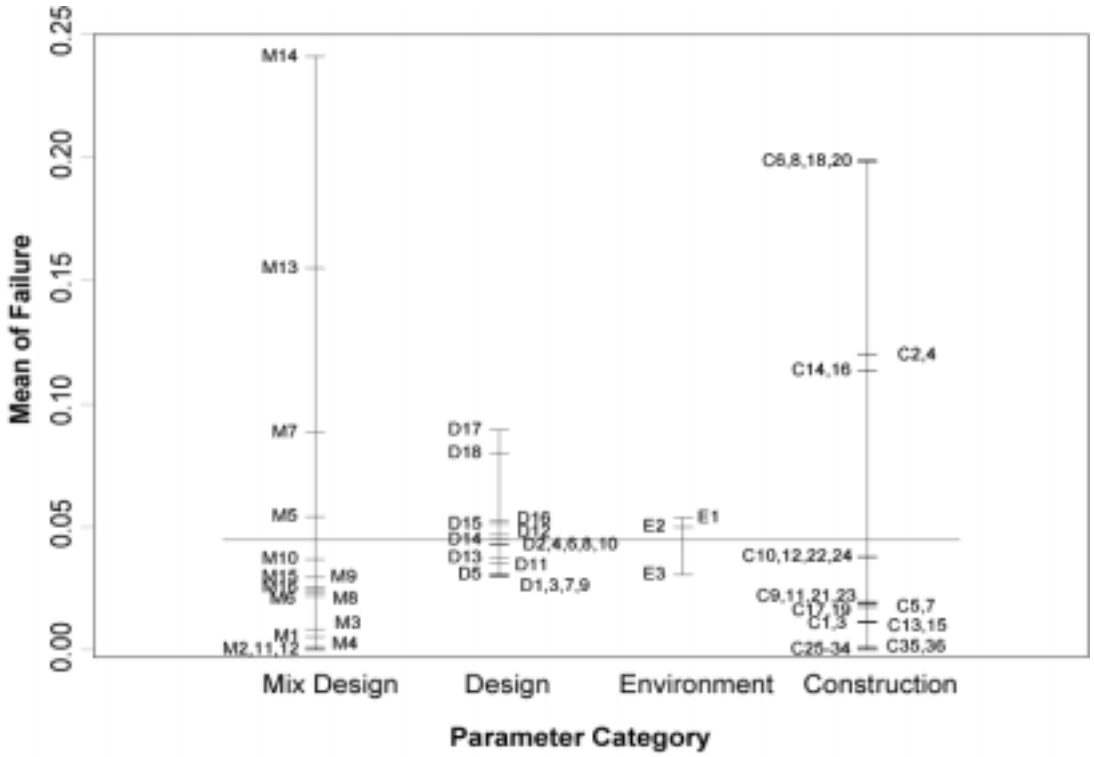


**Figure 22. Relative sensitivity of the Failure mode analysis to the four parameter categories, overall California case.**

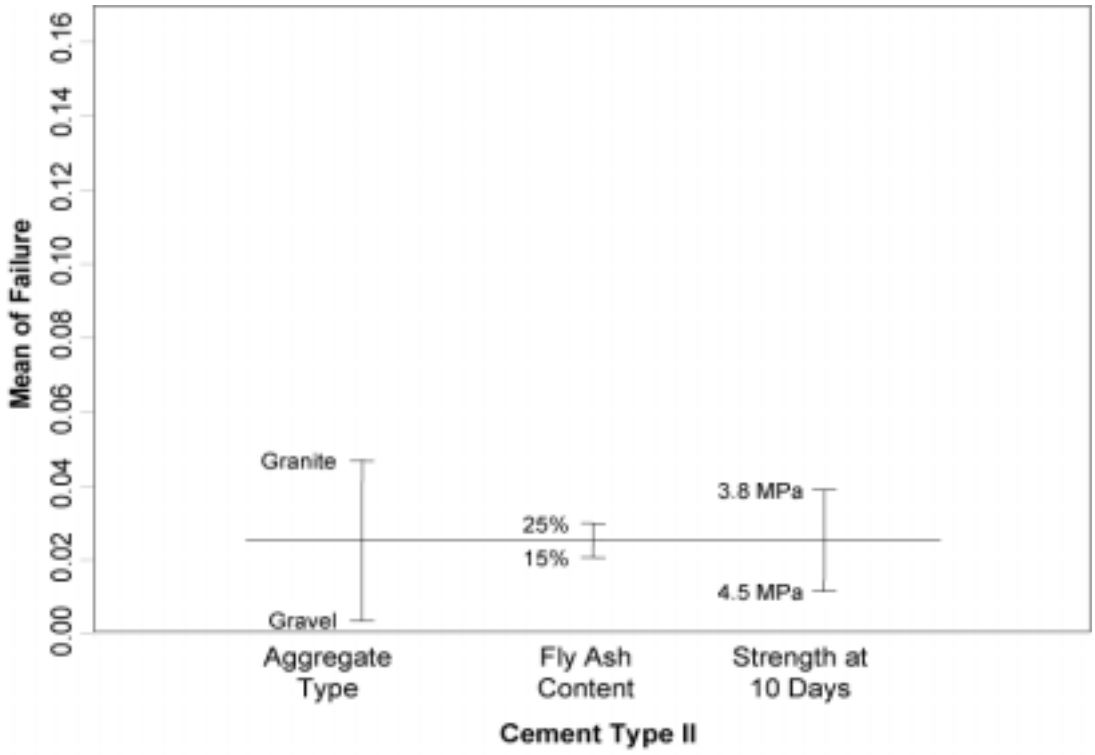


**Figure 23. Effects of Type II cement mix design parameters on Failure mode analysis for overall California case.**

analysis. However, the relative sensitivities are similar.

Note that some of the Failure mode analysis figures show different trends than the respective figures from the Ratio mode analysis. One example is Figure 24—unlike the result from the Ratio mode analysis (Figure 16) in which fly ash content had very little influence on the results, for this case (mix design parameters, Type III cement), fly ash content is the most significant parameter affecting the results in the Failure mode sensitivity analysis.

This occurs because a large number of the failure cases become non-failure cases when fly ash is used. The switching of even a few failure cases to non-failure cases causes the sensitivity shown in the figure to change dramatically because of the overall very low percentage of failures predicted by HIPERPAV in the experiment (approximately 6 percent, as shown in Figure 24).

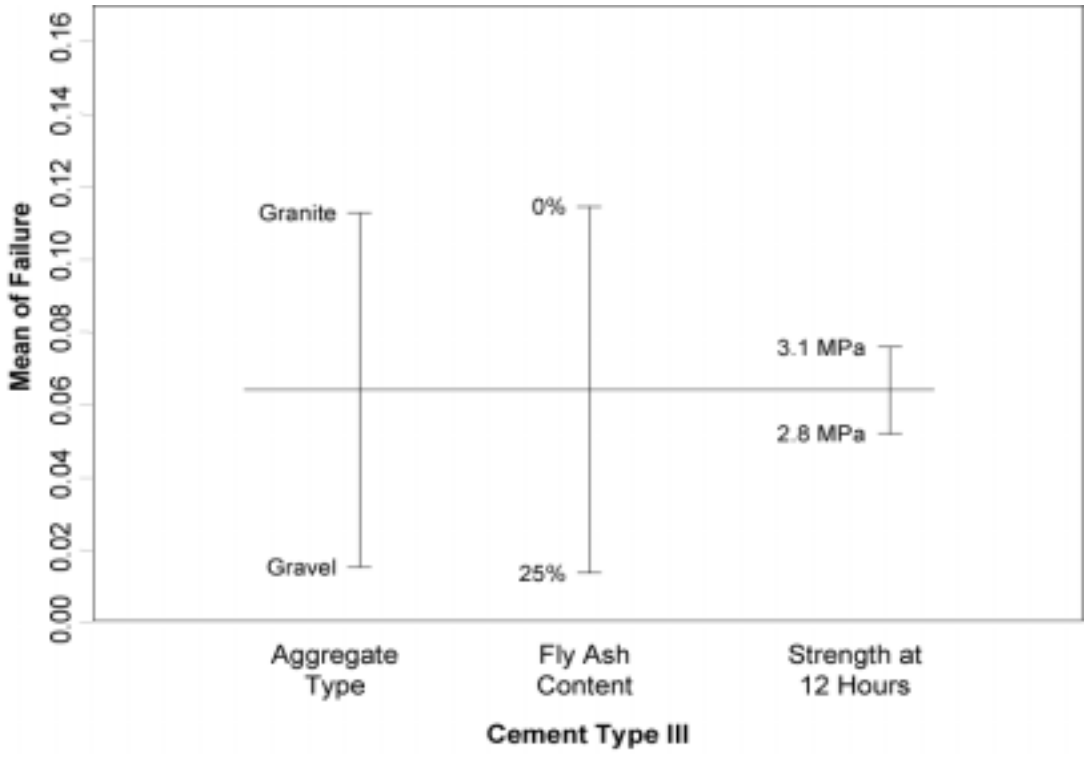


**Figure 24. Effects of Type III cement mix design parameters on Failure mode analysis for overall California case**

# 5.0 CONCLUSIONS AND RECOMMENDATIONS

Because the phenomena involved in early-age cracking in concrete are very complex, the exact prediction of cracking in jointed plain concrete (JPC) is still an open subject for academic research. However, simplified methods based on reasonable assumptions, such as those provided by HIPERPAV, can help the designer to identify critical factors and the best solutions to reduce the risk of failure due to early-age cracking in JPC.

## 5.1 Conclusions

There are two types of analysis that can be performed using HIPERPAV: *Failure mode* analysis and *Ratio mode* analysis. Failure mode analysis gives a simple yes/no result of whether cracking is predicted to occur based only on whether the predicted stress exceeds the predicted strength of the concrete. The Ratio mode of analysis provides an indication of a given solution's relative sensitivity to the input variables, and which decisions result in reduced risk of early-age cracking (greater strength/stress ratio). Ratio mode does not specifically predict whether cracks will occur, but does indicate how a given parameter can be improved. From this point of view, the model should not be used to verify good behavior from the selection of inputs, but should be used to compare different solutions and determine the influence of the parameters on the final performance.

Although HIPERPAV provides accurate qualitative guidelines for a range of certain inputs, it is probably not sufficient for JPC durability prediction. Comprehensive durability prediction includes the effects of mechanical, chemical, and thermal degradations after several days of placement of the concrete.

From the sensitivity analyses presented in this report, HIPERPAV leads to the conclusion that improvement of construction practice has the most significant impact in reducing the risk of

early-age cracking. Specifically, proper joint sawing and curing times are key issues for reducing this risk. Overall, the Desert climate region (Daggett) is much more critical than the two coastal regions (Los Angeles and Bay Area). Mix design factors are not so important for the Desert region (Daggett), while they are quite important factors for the South Coast (Los Angeles) and the Bay Area (San Francisco) regions.

In the Desert climate region analysis, the type of aggregate is the primary mix design factor affecting cracking in the pavement. In this case, using gravel (softer) is much safer than using granite (harder).

In the South Coast and Bay Area regions, the use of gravel aggregate, fly ash (25 percent), and Type II cement, which is coarser and contains more $C_2S$, provides a reduced risk of early-age cracking. Higher ultimate strengths obtained by using a lower water/cement ratio also provide a reduced risk of early-age cracking.

In the South Coast and Bay Area regions, it was found that JPC geometry is not particularly critical for early-age cracking if loading is not applied. Other parameters such as time of day of construction and seasonal factors do not show significant impact on the results.

## 5.2 Recommendations

Based on the research presented in this report, the following recommendation are made.

### 5.2.1 Changes to HIPERPAV

HIPERPAV is limited in its use and applicability for Caltrans. First of all, the range of validity has not been clearly established. Analysis for cases using Fast-Setting Hydraulic Cement Concrete (FSHCC) has not been developed yet and the models have deficiencies for

predicting behavior of Type III mixes. To address these problems, the program application should be extended to FSHCC materials and modeling of autogenous shrinkage.

HIPERPAV software is a deterministic simulation, but there are always risks embedded in the input data. Input data contain variations in measuring, mixing, and so on, and so HIPERPAV should include a more comprehensive probabilistic analysis.

The durability prediction for cumulative damage of the pavement is not included in HIPERPAV. Given that cumulative damage may have a significant impact on early-age cracking, this should be included in the future version.

In order to better fit Caltrans practice, HIPERPAV should allow data inputs specific to Caltrans practice, such as beam strengths. These modifications to HIPERPAV should then be validated.

### 5.2.2 Improve Caltrans Practices to Prevent Early-age Cracking

Given that the Desert region has the most severe problem with early-age cracking, special care should be taken to establish an appropriate design and construction strategy for that region. Among the four main categories of input data, the construction parameters were found to have the largest impact on early-age cracking. Construction practice should be reviewed to ensure proper scheduling of curing and saw cutting of joints during construction.

According to the analysis, aggregate type was the only important mix design variable in the Desert region, so the mix designer should emphasize aggregate type selection. Measurement of coefficient of thermal expansion (CTW) should be considered.

The effect of fly ash content changes depending on the cement type, and so further study should be performed regarding fly ash content. HIPERPAV indicates that the higher strength concrete with lower fly ash content and low water/cement ratio gives the safest result. To

improve mixing, use of superplasticizer is recommended. Smaller joint spacing is safer than larger joint spacing, and the current Caltrans maximum of 4.6 m is a great improvement over the previous maximum of 5.8 m.

Overall, the use of HIPERPAV as a design tool is worthwhile because it provides a good indication of the correct answers to complex problems that can not be solved intuitively. HIPERPAV should not be expected to always predict early-age cracking correctly, however, it does provide guidance in making decisions to reduce the risk of early-age cracking.

## 6.0 REFERENCES


1. Bradbury, R. D. *Reinforced Concrete Pavements*. Wire Reinforcement Institute, Washington, D.C., 1938.

2. Federal Highway Administration. *HIPERPAV Software, Validation Model Summary.* Report available on web site http://www.tfhrc.gov/pavement/pccp/hipemain.htm (no other publication information available for this report on FHWA Turner Fairbanks Highway Research Center web site).

3. Rasmussen, R. O. and B. F. McCullough. *A Foundation for High Performance Jointed Concrete Pavement Design and Construction Guidelines.* Transtec Consultants, 1998, pp. 1-23.

4. Rasmussen, R. O. et al. "Constructing High-Performance Concrete Pavements with FHWA HIPERPAV Systems Analysis Software. *Transportation Research Record.* No. 1813. 2002. pp. 11–20.

5. University of California Pavement Research Center. *Draft Test Plan for HIPERPAV Validation, Concrete Maturity Meters, and Concrete Pavement Instrumentation in District 8*. March 2001.

6. Ulm, F. J. and O. Coussy. "Modeling of Thermo-chemo-mechanical Couplings of Concrete at Early Ages." *Journal of Engineering Mechanics*, ASCE, 121 (7), 1995, pp. 785-794.

   Ulm, F. J. and O. Coussy. "Strength Growth as Chemo-plastic Hardening in Early Age Concrete." *Journal of Engineering Mechanics*, ASCE, 122 (12), 1996, pp. 1123-1132.

   Ulm, F. J. and O. Coussy. "Couplings in Early Age Concrete: From Material Modeling to Structural Design." *Int. Journal of Solids and Structures*, 35 (31-32), 1998, pp. 4295-4312.

   Ulm, F. J., A. Elouard, and P. Rossi. "Modeling of Early Age Concrete Cracking Due to Thermo-chemo-mechanical Couplings." *Fracture Mechanics of Concrete Structures* (FRAMCOS-2), F. H. Wittmann, ed. Aedification Publisher, Freiburg, Germany, 1998, pp. 1443-1458.

7. Roesler, J., J Harvey, J. Farver, and F. Long. *Investigation of Design and Construction Issues for Long Life Concrete Pavement Strategies.* Draft Report for the California Department of Transportation. Pavement Research Center, Institute of Transportation Studies, University of California, Berkeley. September 1998.

8. Heath, A. and J. Roesler. *Shrinkage and Thermal Cracking of Fast Setting Hydraulic Cement Concrete Pavements in Palmdale, California*. Draft report prepared for California Department of Transportation. Pavement Research Center, CAL/APT Program, Institute of Transportation Studies, University of California, Berkeley. December 1999.

9. Harvey, J., J. Roesler, J. Farver, and L. Liang. *Preliminary Evaluation of Proposed LLPRS Rigid Pavement Structures and Design Inputs.* Draft Report for the California Department of Transportation, Institute of Transportation Studies, University of California, Berkeley. September 1998.

10. University of California Berkeley PPRC Contract Team. *Strategic Plan for Partnered Pavement Research.* Strategic plan prepared for the California Department of Transportation. Pavement Research Center, Institute of Transportation Studies, University of California, Berkeley. December 2000.

11. Harvey, J., A. Chong, and J. Roesler. *Climate Regions for Mechanistic-Empirical Pavement Design in California and Expected Effects on Performance*. Draft Report for the California Department of Transportation. Pavement Research Center, Institute of Transportation Studies, University of California, Berkeley. June 2000.

12. Neville, A. Properties of Concrete, 4th and final Ed. New York: Wiley, 1996.

13. National Climate Data Center Web site: http://lwf.ncdc.noaa.gov/oa/climate/climatedata.html